Design and Optimization of Simulated Tubular Tunnel FET Structures for Biosensing Applications

By

Dr. Dereje Tekilu

Dr. Avtar Singh

Dr. Gangiregula Subbarao

Dr. Manash Chanda

A Final Research Report Submitted to Adama Science and Technology University

Adama, Ethiopia
October 2023

ABSTRACT

Biosensors are the analytical device which transmits a biological response into the processable and quantifiable signal. There are two types of methods which are generally used to detect the presence of biomolecules in FET based biosensors i.e., dielectric modulation and gating effect. Within several types of innovative bio-sensing technologies, label free dielectric modulated field-effect transistor (DM-FET) based biosensors stand out because of their appealing properties, including ultra-sensitivity detection, mass-production capacity, low cost of manufacture, low-cost manufacturing and batch testing facility.

To continue the Moore's law, the researcher all over the globe are working on the novel approaches to reach the goal of international technology roadmap of semiconductors. Some of the studies are targeting on the novel device architecture and part of them are exploring for the better controlling over the channel. In this race the tunnel FET and the junction less FET both emerges as a promising candidate for low power applications. According to reports in research, silicon nanotube FETs have a considerable electrostatic gate command over carriers because of the shell-core gate stacking structure. The suggested design has a couple of gates (an inner gate and an outer gate) that are made to regulate the channel from within as well as outside the nanotube, which makes it considerably greater in efficiency than a nanowire FET.

This work simulates and investigates the performance of Dielectric Modulated Tunnel Field Effect Transistor biosensor for low power applications. In particular, total five devices we simulate and observe the electrostatic behavior. Out of them three devices are double gate tunnel field effect transistors i.e., double gate both side cavity (DG-BSC-TFET), double gate drain side cavity (DG-DSC-TFET) and double gate full both side cavity (DG-FBSC-TFET). In all these structures we have taken the ambipolar current as the sensitivity parameter and the sensitivity of DG_FBSC_TFET is best for all the neutral as well as for the charged biomolecules. This is due to the fact that volume to surface ratio in this structure is more compare to the other structures. For K=5 the Sensitivity of FBSC structure is 100 times (10^2) more than DSC structure. Due to the fabrication complexity and low ON-current in tunnel FET based biosensors the Junction less FET based biosensor is studied. A junction-less nanowire tunnel field effect transistor (JLN-TFET) that combines the advantages of a junction-less field effect transistor (JLFET) and a tunnel field effect transistor (TFET) and with a hetero-structure device made of silicon

(Si) and germanium (Ge), an amalgamation of gate engineering and channel engineering is investigated. The modified gate-all-around hetero junction less nanowire tunnel field effect transistor (GAA-H-JLNTFET) performs better. The drain current is taken as the sensitivity parameter. Five different biomolecules sensitivity are measured and found better than the previous published results. The sensitivity to detect the gelatin (k=12) is around 4.5 X 10^4, which one is the good result when compared to the other published data.

Finally, the tubular gate on source-based tunnel FET is investigated for the biosensing application. In this FET based biosensor the micro or nano organism can immobilize at the surface above the source and the gate, interact on the upper wall of the biosensor as well as on the inner part of the tube of the Silicon nanotube transistor. The gate electrode is extended on the source and also extended on the little part of drain. A nano gap is formed on the whole volume of the Silicon nano tube inside as well as the outside of the tube except some part of the drain. The ON current is taken as the sensitivity parameters.

All the extensive simulations are performed using the ATLAS tool from SILVACO TCAD. It has been found that incorporating tubular tunnel FET and gate engineering improves the device's TFET performance and qualifies it for low power and more practical applications.

ACKNOWLEDGEMENT

We would like to express our greatest appreciation to Electronics and Communication Engineering Department, and School of Electrical Engineering and Computing, Adama Science and Technology University, Adama, Ethiopia for giving opportunity and encouragement to propose the research proposal.

We would like to gratefully acknowledge Dr. Teklu Urgessa, Dean, SoEEC, ASTU, Adama, Ethiopia for his continuous encouragement throughout the research work. As well-wisher, his insight, observations and suggestions helped us to establish the overall direction of the research and contributed immensely to the success of the work.

We acknowledge Mr. Tadesse Hailu Associate Dean for research & Technology Transfer, SOEEC, Adama Science and Technology University, Adama, Ethiopia for their support and suggestions during the process of the project.

We acknowledge the academic resource that we received from Adama Science and Technology University, Adama, Ethiopia giving us a comfortable and active environment for pursuing our research work.

Finally, we would like to thank our staff members of the School of Electrical Engineering and Computing for their support and encouragement throughout the research work.

Table of Contents

LIST OF FIGURES

LIST OF ACRONYMS

SCEs	Short channel effects
Si-NTFET	Silicon- nanotube field effect transistor
POCT	Point-of-care testing
POC	Point-of-care
SCE	Short channel effect
DIBL	Drain-induced barrier lowering
TFET	Tunnel field effect transistor
SOI	Silicon-on-Insulator
CNTFET	Carbon nanotube field effect transistor
IMOS	Impact ionization MOSFET
GBP	Gain-bandwidth product
JLT	Junction-less transistor
DM-FET	Dielectric modulated based FET
BTBT	Band-to-band tunneling
DNA	Deoxyribonucleic acid
LOD	Limit of Detection
PSA	Prostate-specific antigen
DM-NT FET	Dielectric modulated nanotube FET
DM-ED-TFET	Doped tunnel field-effect transistor
L-DMTFET	Lateral dielectrically modulated tunnel field-effect transistor
MOSFET	Metal oxide semiconductor field effect transistor
TCAD	Silvaco Atlas technology computer-aided design
DG-TFET	Double gate-tunnel field effect transistor

LIST OF TABLES

CHAPTER ONE
INTRODUCTION

1.1 Background

Many different approaches have previously been put out by many research groups to reduce the short channel effects (SCEs) that the present CMOS technology is subject to[1]. Amongst all of these approaches, procedures focused on gate engineering were discovered to result in MOSFETs with lower short channel effects (SCEs). These gate engineering approaches include things like multi-gate architectures, gate stack configurations, and substituting different materials for the dielectric material [2]. In addition to the methods outlined above, several more novel structures have been suggested and developed by scientists as potential replacements for MOSFETs. Even while it is discovered that the majority of those devices to reduce short-channel effects (SCEs) in a tolerable manner, the cost of this is an increase in manufacturing complexity[3]. Because of an increase in charge sharing from the drain and source, the control of the gate over the channel deteriorates when the channel length is decreased[3]–[6].

Experts from across the world discovered that 3D device architectures such horizontal and vertical double gates, FINFET, and GAA(Gate All Around) structures are better compatible with achieving minimal leakage and excellent performance offered by short channel devices.[7]. One of the most attractive and most appropriate designs for nm technology node transistors is the nanowire MOSFET (which is also referred to the GAA MOSFET) among of all of these semiconductor devices. The excellent electrostatic controllability of the gate over the channel is a significant benefit of the gate all-around structures, primarily due to the gate entirely encompasses the channel through all directions.

The newly developed tubular field effect transistor is introduced for improved control over the gate channel and is referred to as Silicon-Nanotube Field Effect Transistor (Si-NTFET)[8]- [11]. Due to the absence of the body contact or as substrate contact within the tubular architecture, the Si-NTFET body bias effect is less severe compared to that from MOSFET.

There are two types of Biosensors which are generally made with the help of FET based devices. One is using the Gating Effect and the other one is by using the gate dielectric modulation. In gating effect the dielectric material of the gate is interchanged by a thin layer of receptors which fused with the charged biomolecules and the subsequent change in the energy band of the device is recorded and hence, the change in drain current is also noted[12].

In dielectric modulated biosensor the part of the gate material is etched out and make it as a Nano gap; when the neutral or charged biomolecules sit into the gap then due to the change in the dielectric constant of the gate, all the capacitances associated with the gate terminal is varied and due to which the drain current finally increase or decrease depends on the type of biomolecules entered into the Nano gap area. The gating effect is generally used for the detection purpose of charged biomolecules, whereas dielectric modulated based biosensors are used for both type of biomolecules detections neutral as well as charged biomolecules.

First time in 1960s the ISFET(Ion Sensitive Field Effect Transistor) based biosensor was developed by Bergveld[13]after that H. Im et.al, proposed a dielectric modulated biosensor[14]. Further Banerjee and Sarkar demonstrating the nanowire TFET as a biosensor for positively charged biomolecules by utilizing the gating effect[12].

The sensitivity of the biosensor is very much depending upon the filling of the Nano gap region. Partially filled biosensor was studied by Kim et al. and they reported that in practical cases due to steric hindrance the measurement of the sensor is not accurate. Therefore In their work they proposed a parameter fill factor stated as the ratio of biomolecules occupied in the Nano gap region[15].Narang et al. reported identical investigation for partially filled region for dielectric modulated FET [16]. When the Nano gap is partially filled then the response of the biosensor decreases. It is because of the effective dielectric constant changes with the position of the biomolecules in the nano gap region.

It is claimed that FET biosensors were an excellent option for point-of-care testing (POCT) in the coming decade. FET-based biosensors are attractive hopefuls for possible future POCT purposes as opposed to bulkier optical-based IVD equipment because of the benefits of sensitivity, effectiveness, compactness, lightness, low power, plus effortless integration in electronics read-out subsystems[17]. Furthermore, microfluidic sample collection cartridges may be coupled with FET-based sensors to enable fully automated testing operations.

For an illness to be detected and then get the ideal medical treatment, an efficient disease diagnosis needs to be obtained. As a result of their individualized character and unclear link to disease status, the symptoms used to diagnosis many diseases today may result in late discovery or be deceitful. The biological molecules referred to as biomarkers, such as cells, DNA, proteins, peptides, or others, are more intimately associated with the fundamental cause of disease[18]. As a result, identification of an illness may be achieved by monitoring for significant disease biomarkers on a regular basis. As a result, detecting illness biomarkers is critical, providing clinicians with a more objective along with quantitative foundation for making medical decisions. Point-of-care (POC) diagnostic devices offer a realistic way for detecting and analyzing disease-related indicators in a timely and sensitive manner. In comparison to traditional lab apparatus, biosensors are progressively being used as potential diagnostic devices, providing for easy, low-cost point-of-care testing[19].

Bio sensors and biological electronics are technological devices used in biology and health. A biosensor is an example of analytical equipment that consists of a biological part and a physicochemical sensor. Bioelectronics applications include cardiac pacemakers, blood sugar meters, and magnetic resonance imaging (MRI). The electrical engineering, biology, chemistry, physics, and materials science are all part of the topic of Bioelectronics. Electronic devices serve an important role in assessing biological systems and have transformed diagnostic approaches. A biosensor is a device that detects the presence of several compounds in a sample by using biological materials. It's a sensor that combines an element of biology with a physiochemical transducer to generate an electrical signal proportionate to a single analyte that is subsequently transferred to a detector.

Biosensors are instruments that measure either the presence or the concentration of a biologic analytic agent, such as an enzyme, biological structure, or bacterium. Three components make up a biosensor: a portion that detects the analyte and generates an electrical signal, the signal transducer, plus a reading device. Biosensors may be utilized in a variety of applications, such as the processing of food for evaluating food quality, safety, as well as authenticity; fermentation processes and inspection; biosensing methods for environmentally friendly food safety; healthcare field-diagnosis (such as diabetes); fluorescent biosensors (as diagnostic tools to diagnose cancer); biological defense biosensing applications (e.g., defense against biological attacks); and metabolic engineering to monitor cell [19].

Biosensors come in a variety of varieties, including electrochemical bio sensors, optically biosensors, electronically biosensors, electromechanical biosensors, gravimetric biosensors, and pyroelectric biosensors. The layout of electronic biosensors, particularly those based on FETs, is the mainstay of this study. Due to their compact sizes, label-free identification, simple manufacturing method, and widely recognized physics-based justifications, FET-based biosensors are attracting interest.[17].

In this research project, our objective is to build the DM based Biosensor for the detection of the bio-molecules in sub threshold region[20]. Both the threshold voltage (Vth) as well as the on current (ION) of the device change dramatically according to the value of the dielectric constant along with charge nature of the biomolecules, making it possible to detect certain types of molecules. In this research, label-free biosensing using nanotube-based biosensors is suggested and will be implemented in an environment of very low ionic concentration. The biomolecules are confined in nano gaps that were created by etching off the central portion of the gate between the inner and outer gates.[21]. We believe that this project help the medical community by making the testing of the disease more accurate and in less span of time since less time is required for the diagnosis of the diseases.[17][22].

1.2 Statement of the Problem

In order to harvest high-speed integrated circuits with high-packing density, rapid innovations in semiconductor technology having pushed MOSFET dimensions down to the nanoscale regime. Short channel

effects, from the other side, have such a significant impact on device performance in ultra-scaled designs [23]. FET biosensors is addressed to be a good candidate for next decade point-of-care testing (POCT). It is described as a clinical diagnostic test done when a patient requiring medical attention. A glucometer, as the case is utilized at the patient's home or bedside instead of at a central laboratory in hospitals. Its operation must be easy enough for a person with little training or even no training to carry out POCT. Additionally, it significantly reduces the time it takes for test findings to be available, giving clinicians access to accurate information immediately. FET-based biosensors are attractive contenders for future POCT usage as opposed to bulky optical-based IVD devices because of the benefits of sensitivity, selectivity, compactness, lightness, low power, and seamless integration in electronic read-out systems.[17]. Additionally, microfluidic cartridges for gathering samples can be coupled with FET-based sensing devices to provide completely automated testing operation. In Dielectric Modulated Tunnel Field Effect Transistor based biosensor, design, analysis and investigation of the device biosensing parameters are very essential. However, the study and performance analysis of FET based tubular biosensors are not much explored. Hence, in this project work the performance of label-free Dielectric Modulated Double Tubular Field Effect Transistor based biosensor was addressed in order to improve the sensitivity performance of the biosensor and optimize the device architecture for better application. Finally, the performance of the biosensor device analyzed in terms of its energy band diagrams, surface potential, electric field, drain current sensitivity, and ambipolar current by using different device level techniques.

1.3 Objectives

1.3.1 General Objective

Design and analyze the electrical characterization of the split gated silicon nano tube FET and Tunnel FET for the specific detection of micro-organism like various enzymes, protein and viruses.

1.3.2 Specific Objectives

- Develop a self-consistent simulator to calculate spatial charge and electrostatic potential distribution within FET based sensor for biomolecule detection.
- Study the challenges in the electrical characterization of the FET based Biosensor
- Analyze the effect of Nano gap level (filling level) on the sensitivity of Biosensor
- Analyze the effect of short channel effects on the sensitivity of Biosensor.
- Optimize the biosensor for the maximum detection capability.

1.4 Research Contribution

In medical services, physician diagnosis diseases through variety of symptoms, which may cause late detection or be misleading, due to their subjective nature and the uncertain relationship to the disease state. To overcome this problem automated diagnosis tool is needed with best accuracy and less time of disease detection. In this research project we contributed the following to research communities:

- An optimized simulated silicon nanotube FET and TFET biosensors
- The proposed model will be applicable to detect enzymes, antibodies, receptors, organelles and microorganisms for label free bio-sensing. The Biosensor optimized for detection, which is tuned for the following parameters:
    - Drive current
    - Leakage current
    - Subthreshold slope
    - Ambipolar current
- Circuit level approach will be detailed as output for the proper commercialization of the biosensors.
- If the proposed model can be commercialized then the product would be efficacious for the rapid diagnosis of infectious diseases and timely initiation of appropriate treatment would be possible at low cost.

1.5 Significance

For an illness to be detected and then get the ideal therapy, an efficient disease diagnosis is required. As a result of their qualitative character and unclear link to disease status, the symptoms used to diagnosis many diseases today may result in late discovery or be deceptive. The biological molecules known as biomarkers, such as cells, DNA, protein, peptides, or proteins, are more intimately related to the underneath cause of disease. Regularly checking for key illness biomarkers can help in disease diagnosis. Therefore, identifying illness biomarkers is essential since it provides physicians with a more factual and quantitative foundation to evaluate clinical decisions. A practical technique for the quick and accurate identification and assessment of disease-related biomarkers is provided by point-of-care (POC) diagnostic tools. Compared to traditional lab equipment, biosensors are getting employed more and more as potential diagnostic tools that enable quick, low-cost POC testing.

1.6 Project Report Organization

Chapter 1 presents a brief background of label free FET based Biosensor. Some part of vital literature work is also discussed in this chapter, critical literature review on research work reported on different segmentation and merits and demerits of different FET structures based biosensors, objective and significance of the study followed by statement of the problem.

Chapter 2 presents the detailed literature review on tunnel FET, junction less tunnel FET, Tubular tunnel FET and finally on the biosensors

Chapter-3 presents the detailed description of the device structures and also the simulated models utilized which were employed in this project work are presented. Finally, different types of devices which are utilized for the simulation of biosensor are explored

Chapter 4 presents the results of FET devices and simulated tubular biosensing device. In this chapter several architecture of tunnel FET, including tubular tunnel FET are discussed. Further different types of biosensors based on the area exposed for the biomolecules to immobilize are presented. The junction less tunnel FET based biosensor, source engineered biosensor are also discussed.

Chapter 5 presents the conclusion for the research work followed by reference. It also focuses on contributions of the project and future scope.

CHAPTER TWO
LITERATURE REVIEW

2.1 Overview

The development of integrated circuit technology has brought a new era of electronics with tremendous computational capacity. The most typical MOSFET dimensions have continued to be decreased by research and development efforts in the electronics community over the past few decades, enabling better circuit densities and greater functionality at lower prices. The co-founder of Intel, Gordon Moore, anticipate that semiconductor chips would double in power every two years and eventually shrinks to the point that they could be installed in the building, vehicles, and mobile devices [3], [24].

With the resource provided by recent development in the semiconductor industry different techniques investigated for further reducing the size of transistor density and improving performance. The MOSFET's performance is limited to different scaling issues, such as drain-induced barrier lowering (DIBL), short channel effect (SCE), Velocity saturation, etc[25]. Scaling down MOSFETs devices channel length and oxide thickness decrease while substrate doping increases (Dennard scalability). However, due to DIBL and SCE channel length and oxide thickness-scaling technology experienced increasing in I_{OFF} (Leakage current). The requirement of low power and physical constraints on feature size with MOS technology have a direct impact on the peak operating frequency. Extensive pursuit for novel devices and new materials have increased in recent years. Emanated novel structures like, Silicon-on-Insulator (SOI), Fin-FET, Tunnel field effect transistor (TFET), Carbon nanotube field effect transistor (CNTFET), spin-based device, Nanowire FET, ferromagnetic logics [3], [26]–[28], junction less FET were introduced to overcome the limitations of conventional MOSFETs. Different techniques with channel engineering and gate engineering were employed to improve these device characteristics. Some of these structures are discussed below.

2.2 Multi-Gate Structures

The major problem faced by semiconductor industry is how to maintain a controlled flow of charge carriers in the channel with an increasing value of drive current at reduced channel lengths. To mitigate this issue multiple gate devices were evolved to have a better electrostatic control over the channel at reduced length. In the year 2003, the Fin-FET with DG-MOS was first presented by T Sekigawa and at.al [29]. By using this structure, a better control over the channel depletion region was obtained as compared to SOI FET. Specifically, the impact of the drain induced electric field on the channel is reduced, because of which DIBL and other short channel

effects are minimized [25] A different cutting-edge device design for MOSFET scaling problems is the FINFET [30]. It has a thin-body non-planar MOSFET constructed on silicon-on-insulator (SOI) or bulk substrate, using patterning and etching technologies. In Fin-FET, the SS (Subthreshold Swing) improved (i.e., close to 60 mV/decade at room temperature), and SCE can optimize the fin size. Massive scaling of Fin-FET is identified as a device that maintains better AC performance and high switching rates when compared with MOSFETs [31]. Fin-FET provides an opportunity for researchers in other devices due to the fabrication difficulty. A lot of research has also been done on gate all around FETs (GAAFETs). The electrostatic control they offer is excellent. However, there are complicated fabrication aspects to the stacked-FET technology, such as creating a fin structure with a large aspect ratio [32]. The devices on some new transport phenomena explored to replace conventional MOSFETs. An Impact ionization MOSFET (IMOS) and tunnel field-effect transistor (TFET) [33] are a few devices that exploit impact ionization and band to band tunneling, correspondingly, as novel phenomena for carrier transport. Due to their remarkable leakage power efficiency and low OFF current, TFETs have received much investigation for low-power VLSI circuits. The high voltage necessary for impact ionization causes IMOS to deteriorate [34]. To enhance the ON-current per unit area, multiple gates all around channels can be stacked on top of one another, while gate, source and drain are shared. From the fabrication point of view, among all promising CMOS device structures, the silicon nanowire MOSFET (Si NW) is found to be an advantageous as it is made up with silicon, the cheapest raw material that the semiconductor industry has been working from last five decades. It would be really attractive and profitable to remain with the silicon and also achieve better device performances at nanoscale.

2.3 Tunnel FET and its Evolution

The concept of TFET was first given by Stuetzer in 1952 before the emergence of Esaki tunnel diodes, when he developed a p-n junction and that given their principle of operation under reverse bias condition [35]. It was termed as ‘fieldistor’. It discussed about the impact of the particular position of the control electrode on device performance, show the presence of ambipolarity in the device characteristics. In 1977, Quinn et al. [35] suggested the idea of surface tunnel junction by replacing the degenerate n-doped source of a conventional MOSFET by a highly degenerate p-doped source. The primary focus of the paper was sub band disband near to the tunnel junction, and the liberty of deciding the phenomenon experimentally. In 1987, Banerjee *et al.* [36] displayed a three terminal device and reported the presence of Zener tunneling in the device. The researcher calculated the tunneling current by resembling the shape of the tunnel potential barrier as triangular. Mostly the scaling issues are observed and stressed on the negligible short channel effects associated with the ‘Silicon quantum device’. In 1992, Baba [35]suggested the surface tunnel transistor (STT), a substitute of Quinn’s

device where he discussed on the utilization of gate to control negative differential resistance (NDR) in forward bias state. In 1995, Amartunga and Reddick proposed gate governed p+-*p*-*n*+ structure of STT, and developed experimentally and through simulation findings to explain band to band tunneling in STTs. They also displayed the conventional formula to find the barrier height at the tunnel junction, which was used in analytical modeling of TFETs[37]. In 1996, Uemura and Baba [38]first showed the negative differential resistance (NDR) in to the two planar-type surface tunnel transistors based on GaAs and InGaAs. After one year they worked on multiple junction version of their proposed tunnel based transistor to obtain the multiple NDR characteristic. The vertical TFET was proposed by Hansch *et al.* in 2000[39]. Finally in year 2004, the first Silicon-on-insulator TFET was proposed by Aydin *et al.* [35]. Further Boucart and Ionescu had given the concept of the Double Gate Tunnel FETs [40] by deploying two gate terminals: one on the front end and the other on the back end, thus increasing the controlling capacity on the tunnel junction. The limitations of TFETs are their I_{ON} compared to ITRS requirements and the stringent fabrication steps necessary for extracting performance. Tunneling occurs in the lateral direction from the source to the channel in a conventional lateral TFET. Point to point (P-P) lateral tunneling refers to this type of tunneling. However, the BTBT (Band To Band Tunneling) can be started vertically and from the bulk to the surface if sufficient gate to source overlap is provided. Line tunneling or vertical tunneling[41] are terms used to describe this type of tunneling. Doping optimization (retrograde doping, pocket implant source etc., [9]. This BTBT is a significant necessity of the energy band steepness, which the device's doping profile can control. In TFETs, an n+ pocket implant near by the source region is typically used to increase the drive current. However, the leakage current also rises significantly because the SRH electric field enhances recombination. Generally, to solve the MOSFETs and conventional TFETs issues, recent literature has proposed tunnel field-effect transistors (TFETs). Tunnel field-effect transistors (TFETs) have a low subthreshold slope, are rare, and are being observed for different type of low power applications. Tunneling between the valence band of the source and the conduction band of the channel occurs in a gated control PIN diode and the gate voltage controls [42]. The gate voltages alter the thickness of the tunneling barrier at the source /channel junction. Esaki observed the tunneling mechanism in the Tunnel diode in 1960. TFETs can operate at a much lower voltage than MOSFETs and, hence, consume less power than MOSFETs [33]. The advantages of TFET are low sub-threshold current, which leads to low leakage per device, and its high I_{ON}/I_{OFF} ratio can be suitable for analog/RF applications. The main challenges in TFETs are the low ON-state current (I_{ON}), leakage current (I_{OFF}), and ambipolar conduction, which reduce the performance of devices. Because when TFETs have a low ON current and ambipolar behavior, there is more delay in the circuits [43]. Due to this low sub-threshold current, it leads to low leakage per device, and the TFET's high I_{ON}/I_{OFF} ratio makes it suited for analog/RF applications have been published recently to increase the efficacy of TFETs, despite the fact that the most of academic studies have concentrated on TFETs for low-power switching applications. As a result,

various attempts are being undertaken all across the world to suppress ambipolar conduction and improve $I_{ON,}$ including the: heterojunction source [44], a high-k gate dielectric [45], a double-gate architecture [46], Ge source TFETs [46], a material with a low bandgap in the tunneling area [47], gate overlapped TFETs (Vertical tunneling TFETs) [31], pocket doped double gate structure [48], extended source TFETs [49], and L-shaped TFETs [50] have been used to enhance ON-state current.

All of the approaches discussed above considerably improve the drive capability of TFETS; nevertheless, the ambipolar current as well as leakage current are not improved; this is a limitation of TFETs that degrades the analog/RF functionality of the TFETs. Minimal subthreshold swing (SS), reduced ambipolar conduction (leakage current), and an elevated ON-state current (I_{ON}) to OFF current (I_{OFF}) percentage all represent desirable characteristics for minimal-power switching as well as analog/RF circuits, including a gain-bandwidth product (GBP), transconductance (g_m) and high cut-off frequency parameters [50]. Researchers have documented various efforts in the literature to improve the TFETs parameters.

2.4 Junction Less transistors

The concept of the Junction-less transistor (JLT) is explained in [51] The junction-less transistor is a device that characteristic lacks a P-N junction, and no doping concentration gradient. It makes the manufacturing of transistors smaller than 10nm easier. To say the device is junction-less two condition needs to be satisfied: first, the whole regions should be doped with a high uniform doping concentration and second, the channel thickness must be within 10 Nanometers (nm). Authors in [52][45] have proposed a SOI Hetro-Junction-less Tunnel FET for ultra-low power switching applications. They used HfO2 as gate dielectric and the doping concertation used is 10-18cm^{-3}. They investigate transconductance (g_m), and output conductance (g_d). They have found I_{ON} ~0.23mA/µm I_{OFF} ~2.2x10^{-17} A/µm, I_{ON}/I_{OFF} of ~10^{13}, V_{th} of 0.11V DIBL of ~93mV V^{-1} subthreshold slope (SS) ~12 mV/Dec. Author in [53], has proposed an asymmetric Junction less nanowire they have used a dielectric pocked between and source and channel interface without the need for any separate implantation or epitaxial growth. The source side n+ pocket provides a reduction of tunneling width at the source-to-channel interface when the device is in on state.

Authors in [54], have proposed Junction-less nanowire TFET using Hetero-gate-dielectric. They have induced a local dip in the conduction band edge at the tunneling junction which creates an abrupt transition between the on and off-states. They have used platinum (Pt) contact region to convert the n+ doped region into P+ region with a 5.93eV work function on the source side. They have used non-local band-to-band tunneling (BTBT). The difference between the high-k and SiO_2 creates a band diagram modification. A uniform doping concentration of 10^{-19} cm^{-3} and achieving a subthreshold of 45 mV/Dec, I_{ON} 8.6x10^{-6} Aµm^{-1} I_{OFF} 1.1x10^{-11} Aµm^{-1}, ION/IOFF of ~15 .

Author in [55] have proposed a Heterostructure, which contains a different material source and channel drain, without any metallurgical junctions between them. The device has a control gate (C_g) and Auxiliary gate. The doping concentration is 10^{-19} cm^{-3} through the source to channel-drain. They used hafnium oxide, and SiO_2 as gate oxide and spacer respectively between the control gate and auxiliary gate. Aluminum is used for the control gate with work function of 4.2eV and platinum for auxiliary gate work function of 5.2eV.

Authors in [56] have proposed a double gate Junction less Tunnel field effect transistor. They investigate a double gate, which uses two gate two isolate (control gate and polar gate) that uses two different work functions to make it behave like TFET. In the simulation they have used a high-k material which is TiO_2 and with gate length of 20nm. They have obtained subthreshold slop (SS) of ~38mV/Decade, I_{ON}/I_{OFF} ratio of ~$6x10^8$.

Author in [57] has proposed A junction less double-gate TFET using a charge plasma concept which forms a source and drain region without doping by choosing appropriate work function. For both drain and source electrodes. They study the threshold voltage, as the length of the channel is almost zero. They found a subthreshold slope of 56.7mV/decade with a channel length of 50nm

2.5 Biosensors

Biosensors are becoming increasingly significant in human life as technology advances, and their widespread usage has restricted efforts by scholars to discover alternative methods for comprehending biomolecules [58]. Due to their good detection ability, low-power conception, low cost, label-free molecule identifications dielectric modulated based FET (DM-FET) have drowned interest. However, as their technology advanced the device dimensions are scaled down which led to problems like short channel effect (SCE), off state leakage current redaction, high power dissipation which make in degradation of DM-FET. So, to address the above issues, different researchers proposed TFET based biosensors which work on the principal Band-to-band tunneling (BTBT) which allows the device, lower power dissipation, its steep sub-threshold swing (SS), High sensitivity, and quick response time. Since TFET encounters a very sharp doping profile at the Junction the device fabrication complexity and cost are increased.

A biosensor is a device that generates signals proportional to the concentration of an analyte in the given reaction by measuring biological or chemical reactions of the analyte. A typical biosensor consists of the following components [59].

• **Analyte**: A material of interest that must be identified. Glucose, for example, serves as 'analyte' in a bio sensor intended for identifying glucose.

• **Bio-receptor**: A bioreceptor is an organic compound that identifies analyte individually. Bioreceptors include proteins, tissue cells, the aptamers, a type of DNA, and antigens. Bio-recognition refers to the process of signal creation (in the form of light, heat, pH, charge or mass shift, etc.) that occurs when the bio-receptor interacts with the analyte.

• **Transducer:** A transducer is a component that transforms one type of energy to a different one. The transducer in the biosensor converts the bio-recognition signal into a quantifiable signal. This kind of energy conversion procedure is called as signalization. The majority of transducers provide optic or electronic signals that are proportionate to the number of analyte-bioreceptor couplings.

• **Electronics:** This is the section inside a biosensor which processes and produces the transduced information for display. It is made up of complicated electrical circuitry that provides signal conditioning functions such as amplification and signal exchange from analog to digital. The analyzed signals are then evaluated through the biosensor's display module.

• **Display:** This is the section of a sensor that analyzes the transduced information and presents it for display. It is made up of sophisticated electrical circuitry that provides signal conditioning functions like amplification as well as signal transformation from analog to digital. The biosensor's displaying unit quantifies the analyzed signals.

2.6 Characteristics of Biosensor

The following are the most important attributes of Biosensor. The optimization of these attributes is reflected on the performance of the biosensor [59].

Selectivity

The capacity of a bio-receptor to detect a certain analyte in the presence of various admixtures and pollutants is referred to as selectivity. When designing a biosensor, selectivity is the most important factor to consider when selecting bio-receptors.

Reproducibility

Reproducibility is the capacity of the biosensor to deliver same results for a recurrent test setup. The transducer and circuitry of a biosensor are what give it its high degree of accuracy and precision. Whenever a sample is tested multiple times, accuracy refers to the sensor's capability to offer a mean value that is near to the real value while precision refers to the sensor's ability to produce identical findings every time. The inference built on a biosensor's responses is very reliable and robust when the signals are repeatable.

Stability

The level of susceptibility to environmental instabilities inside and outside the biosensing system is known as stability. The signals that come out of a sensor under measurement may acquire a sense as a result of all of these instabilities. This may result in an inaccuracy in the level being detected and may compromise the biosensor's accuracy as well as precision. The crucial quality for a biosensor in applications requiring for prolonged incubation times or continuous monitoring is stability. Responses of electronics and transducers could be

sensitive to temperature, which might affect a biosensor's reliability. To achieve a steady response from the sensor, proper tuning of the electronics is necessary. The degree to which the analyte attaches to the bio-receptor—the affinity of the bio-receptor—can also have an impact on stability. High affinity bio-receptors promote the analyte's covalent or strong electrostatic connection, which enhances the stability of a biosensor. The degradation of the bio-receptor over time is another element that influences a measurement's stability.

Sensitivity

Sensitivity, also known as Limit of Detection (LOD), refers to the lowest concentration of analyte that the sensor can identify. In many clinical and environmental monitoring applications, a biosensor is needed to confirm the presence of amounts of analytes in the specimen at concentrations that are as low as ng/ml or even fg/ml. For instance, prostate cancer is linked to blood levels of the prostate-specific antigen (PSA) of 4 ng/ml, for which doctors recommend biopsy procedures. As a result, sensitivity is thought to be a key characteristic of a biosensor.

Linearity

The characteristic of a biosensor known as linearity demonstrates the precision of the observed response to a straight path for various tests at various analyte levels. Mathematically, it is written simply $\boldsymbol{O = S*Ca}$, wherein Ca is the analyte's concentration, O represents the output signal, and S indicates the biosensor's sensitivity. The sensitivity of the biosensor and the range of levels of analyte being tested can both affect the biosensor's linearity. The smallest change in an analyte's concentration necessary to cause a change in the biosensor's response is known as the resolution of the biosensor. Depending on the application, a strong resolution is needed since many biosensor applications call for not only the identification of analytes but also a measurement of their concentrations throughout a broad operating range. Linear range, another word for linearity, is a range of amounts of analyte in which the sensors response alters linearly along with concentration.

2.7 Biosensors Applications

There is a huge variety of ways that biosensors may be applied to improve quality of life. This includes using them to monitor the environment, find diseases, ensure food safety, defend, find new drugs, and other things.

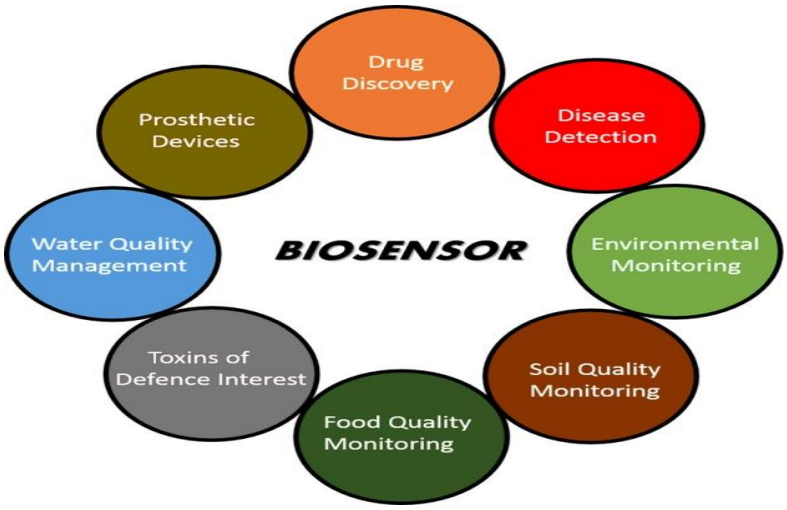

Fig.2.1 Biosensors application Areas [59]

2.8 Types of Biosensors

Biosensors are classified into two groups i.e., either based on the Bio-receptor used in the analysis or the method of transduction implemented. Some of the commonly used biological elements or bio-receptor elements are:

- Immunosensor,
- Nucleic Acid Based,
- Aptamer based,
- Cell based,
- Biomolecule based,
- Biomimetic Based

The next and most popular method of categorizing biosensors is based on the kind of transduction that is employed within the sensor, or the kind of physiochemical that is produced as a consequence of the detecting event. These are:

- Thermoelectric Biosensors
- Optical based Biosensors
- Electrochemical Biosensors
- Piezoelectric Biosensors
- FET Based Biosensors

Again, just a few subclasses exist for each of these categories. An extensive list of several Biosensor types is shown in the accompanying picture (Fig. 2).

Fig. 2.2 Types of Biosensors

2.9 Biosensing Concept

Biosensors generally consists of three components namely: Biological sensitive probes that used to identify target elements, Transducers that used to convert the concentration of the target element into readable signals (optical, electrical or magnetic) and Amplifier that used to amplify detected signal. One category of FET based biosensors which is also called Bio-FETs. Bio-FETs use MOSFET structure and gated by changes in surface potential induced by binding molecules [60]. The gate metal of MOSFET is replaced by Ion sensitive

membrane, electrolyte solution or reference node. The change in surface potential on sensitive membrane brings change in charge distribution which in turn results in change in electrostatic surface potential. The change in electrostatic surface potential will cause change in current in the channel. In conventional FETs gate voltage is altered by external power sources while in Bio-FETs it is changed by concentration and species of biomolecules that are chemically conjugated on the gate. Measuring this change of current is equivalent to target element or electrolyte detection [61]. Additionally, even in complicated biological systems, signals may be efficiently converted into electrical signals as well as amplified by changing various electrical output parameters like mobility (μ), threshold voltage (Vth), on and off ratio (Ion/Ioff), and source-drain currents (Ids). This enables the quantitative identification of biological things [62].

Unlike electrochemical sensors the Bio-FETs without any labeling or expensive manufacture, they are capable of having excellent sensitivity and selectivity. Additionally, the Bio-FETs offer affordable, portable, simple, individualized, and everyday diagnosis without the need for cumbersome measuring equipment. The ability of Bio-FETs to act as an inherent amplifier, transforming minute variations in surface potential into significant variations in current (by the transistor component) without the need for extra circuitry, is another benefit of these devices. They are therefore smaller and more reasonably priced. Bio-FETs are compatible with existing planar techniques for large-scale circuits and have low weight and mass production costs. They are simple to include into Lab-on-a-Chip digital microfluidic devices.

From three main components of biosensors two of them: Biological receptor and transducer are very important in Bio-FETs since the third one which is amplification can be done by the transistor itself. The biomedical receptor converts analyte concentration into chemical or physical output signal with a defined sensitivity whereas the transducer generates electrical signal from chemical or physical output signal. In order to fabricate biosensors, the design of transducer structure and selection of novel materials for transducer design and synthesis of compact bio-receptor has to be considered. The authors in [62], have reviewed and summarized the progress development of bio-FETs transducers and bio-receptors for biomedical applications.

Even though Bio-FETs showed better selectivity & sensitivity and has lower cost when compared to electrochemical biosensors, their application can’t go further due to their inability of detecting neutral charged particles. Hence to overcome this issue, Dielectric Modulated (DM) FET based biosensors are introduced [63]. In Dielectric Modulated FET based biosensors, cavity is created a nanocavity is created underneath the gate electrode, which is subsequently stuffed with biomolecules. Because various biomolecules have varying dielectric constants, the cavity's dielectric constant fluctuates. Additionally, the device's electrical properties change, which is reflected in variations in the transfer curve and sensitivity [62].

Different applications like biomedical diagnosis and point of care testing requires a miniaturized and light weight biosensor. The development of such miniaturized biosensing technology becomes visible with the

advent of nanotechnology. Nanotechnology deals with use of nanomaterials and design of nanoscale devices and systems. Nanomaterials have a very special features like high surface area to volume ratio, biocompatibility, high sensitivity and good chemical stability. Hence the use of such materials and the technology has crucial advantages in biosensor design and development like the improvement of sensitivity due to the high surface area to volume ratio. With the advent of nanotechnology Nanowire and Nanotube based biosensors are designed in order to benefit from Nano technology design. In addition, the design of Nanowires and Nanotubes will help to overcome the Short Channel Effects that is caused due to shrinking of MOSFET dimensions to nanometer scale following the Moore's law. Due to their increased gate electrostatic controllability and improved ability to suppress short channel effects (SCEs), they provide enhanced device functioning. In compared to its planar and multigate counterparts, 1D channel geometrics with nanotubes or nanowires that are wrapped entirely around gates provide the highest controllability for the channel and the best Ion/Ioff ratio. Both Nanowires and Nanotube based biosensors can be designed using bio-receptor and Dielectric modulation methods [21]. In this project, we mainly focus on Dielectric Modulated Nanotube FET (DM-NT FET) based biosensors design.

2.10 FET based Label Free Biosensor

The need for FET-based biosensors had stimulated the improvement of TFET as dielectric modulation biosensors, in which the dielectric constant, as well as the charge of biomolecules in the Gate dielectric region, alters the drain current[64]. Although several TFET architectures have been theoretically explored for dielectric modulated label-free biomolecule sensing, no specific study on construction of a TFET based dielectric modulated biosensor had been documented. TFET-based dielectric modulation sensors, on the other hand, had been researched by a number of experts [19]. Similarly Tunnel Field Effect Transistors have appeared as is among the most important significant devices for, because of its low energy consumption ability to survive the effect of scaling, slow cost and easy operations, Dielectric modulation is applied in biosensor [65].

The FET base biosensor had fascinated a lot of consideration in the sphere of medicine, diagnosis, and environmental security protection in the current setup. The FET-based biosensor has been found to be useful in the healthcare industry, pollution monitoring, and biological pathogen treatment. As the tremendous scaling process continues, CMOS technology with conventional MOSFETs faces a number of challenges, including increased leakage current and a steeper subthreshold slope (SS). In [66], Tunnel field effect transistors that use a band-to-band tunneling technique were predicted to increase leakage current and SS limits. The goal of this article is to build a DG underlap-TFET structure for biosensors with low leakage current, subthreshold, and sensitivity. Asymmetry between source and drain, as well as step channel thickness, must be implemented using 2D Atlas device simulator software to further overcome the ambipolar current. The sensitivity (I_{ON}/I_{OFF}) of 10^8

eV/dec is obtained using the band-to-band tunneling model, which is a good result. The channel is p-n-n, and if it's a TFET, it has to be p-i-n, and the electrical parameters are just simulated in this study.

A short-gate TFET (SG-TFET) architecture was investigated for dielectrically regulated biosensing purposes in contrast to a full-gate TFET structure with a similar size [67]. Utilizing sophisticated device-level simulation tools, the sensing performance of Band-to-band tunnelling was used to study both charged and charge-neutral biomolecules, as well as the effects upon the biological molecules dielectric value and charge density. In this study, the DM-TFET of the SG-TFET was compared towards the FG-TFET, and indeed the DG-TFET based biosensors reported a high drain current sensitivity of 10^8 at k=4.

In [66], DG-TFET was projected to overcome the outflow current and subthreshold slope issues. Using the SILVACO TCAD 2D simulation, the performance of DG-TFET with step channel thickness (SC-TFET) was examined. The ambipolar tendency is expected to be comfortable because to the asymmetry between source and drain created with the stage channel thickness. When likened to the conventional DG-TFET, the SC-TFET offers a considerable reduction in ambipolar current. The mechanisms of SC-TFET were closely researched in order to have a better understanding of the structure's physical properties. SG-TFET had an SS of 44.8 mV/dec, whereas typical DG-TFET had an SS of 50.6 mV/dec. To lower the series resistance, the source region is highly p-doped (10^{20} atoms/cm^{-3}) while the drain region is heavily n-doped (10^{20} atoms/cm^{-3}). The channel region is highly n-doped (10^{17} atoms/cm^{-3}). Tunnel field effect transistors were the subject of contemporary research in device structure. It must be generated from p-type-channel source and n-type drain, but both channel and drain are strongly doped n-type in this work, thus this isn't recognized.

In [23], a new dielectric modulated dual material gate nanowire Junction less MOSFET's potential as a capable biosensor was already demonstrated. The impact of structural parameters on the sensitivity of the proposed device was carefully implemented using a 2D device simulator to design a low-power, highly responsive biosensor, and a nanogap was inserted in the gate insulator section to immobilize the biomolecules.
The gate capacitance was modified as biomolecules accumulated in the nanogap, resulting in a threshold voltage variation. Streptavidin (k=2.1), 3-aminoppropyltriethoxysilane (APTES) (k=3.57), and protein (k=8) were the biomolecules studied in this work. As a result, for the doping concentration, an optimum value of doping $3x10^{18}$ cm^{-3} up to $5x10^{18}$ cm^{-3} was attained.
By modifying the gate work function difference over the nanogap area and the remnant part of the channel, the biosensor's sensitivity could be improved for a varied range of biomolecules, and were got $10^8 cm^{-3}$.

In the field of label-free biosensors, fabrication constraints and costs of nanoscale devices was a key concern. As a consequence, a dielectrically modulated electrically doped tunnel field-effect transistor (DM-ED-TFET) was proposed as a biosensor for label-free detection to solve these difficulties [68]. For sensing biomolecules, a nanogap cavity embedded inside the gate dielectric was produced in the proposed work by

etching a specified fraction of the gate dielectric layer towards the source side. The sensing capabilities of the DM-EDTFET were investigated in terms of dielectric constant and charge density of biomolecules, as well as device geometrical characteristics, under various bias situations. In terms of sensing properties, the proposed DM-EDTFET was compared to a MOSFET-based biosensor to determine relative sensitivity. Due to the obvious increase in dielectric constant of biomolecules, there was a large increase in drain current sensitivity, which reached 10^9.

In [69], biosensors constructed on field-effect transistors (FETs) are particularly popular for label-free detection and was also compatible with CMOS technology. High subthreshold swing (SS > 60 mV/decade) and a long response time was two major problems for FET-based biosensors. Tunnel FET (TFET) based biosensors can eliminate this problem because TFET has an SS of less than 60 mV/decade due to its BTBT mechanism. Based on this concept, a vertical dielectrically modulated TFET (V-DM-TFET) as a biosensor was analysed and compared to a lateral dielectrically modulated tunnel field-effect transistor (L-DMTFET) just utilizing underlap mechanism and gate work function engineering in this paper. Charged and neutral biomolecules are deposited in cavities separately to test these devices' sensing capacity. After comparing the suggested structure towards the L-shaped DM-TFET for biosensor applications, the Vertical DM-TFET scored sensitivity of (10^9). The authors in [70], they came up with the idea of a Silicon Nanotube FET, wherein core-shell gate accumulates assisted in achieving full volume inversion by causing an increase in minority concentrations of carriers close to the extremely thin channel and, simultaneously, causing a rapid roll-off at both drain and source intersections, resulting in exceptional performance every device with effective space usage. Furthermore, they demonstrated that both the gate-all-around nanowire FET and traditional planar metal oxide semiconductor MOSFET are inferior to core-shell gate stacks for controlling short channel effects. The authors in [71], have examined how well a strained silicon channel performs in a silicon nanotube FET (Si-NTFET) device. They discovered that the driving capacity as well as inversion charge density for strained Si-NTFET is significantly greater than those of Si-NTFET. The DIBL and additional SCEs are also either decreased or stay unchanged, as they have further verified. The researchers in [70], have for the very first chance in research suggested a split gated silicon nanotube field-effect transistor (FET) biosensor enabling the label-free identification of the microorganisms. They conducted a sensitivity study by taking into account half-filled and full-filled nanogaps using neutral or charge biological molecules within the cavity, and they discovered that the recommended biosensor had a large sensitivity and outstanding short-channel impact mitigation. In this research, we have investigated a novel Dielectric Modulated Silicon Nanotube FET biosensor structure with better sensitivity and reduction of SCEs. In the next subsequent chapter, we have designed several FET based biosensor structures which included tunnel FET, Tubular tunnel FET and junction less FET for better low power performance and also presented the detail investigation of the proposed biosensors in terms of sensitivity.

CHAPTER THREE

SIMULATION METHODOLOGY AND DEVICE STRUCTURE

3.1. Overview

This section lists software requirements, simulation parameters, simulation flow chart, device structure, design parameters, circuit-based simulation, and comparisons of the device structure of TFETs.

3.2. Materials Requirement (Software)

- Silvaco Atlas technology computer-aided design (TCAD) simulation software (version of 5.0.10.R)
- S-Pisces/Mixed Mode
- Origin software V8.5 build number 8.500161
- Visio 2021 software

Simulation of this project work and device structure can be performed using Silvaco Atlas TCAD simulator software (tool). It is used for simulating and graphical analysis characterizing. The different device parameters have been analyzed using the Silvaco Atlas TCAD device simulator. Origin software is used for graph (data) analysis, Visio software is used to draw the device structure and flow chart, and another important tool is mixed mode, which is used for circuit-based simulation or inverter simulation.

3.2.1 Simulation Software Description

The Silvaco Atlas TCAD is a one-, two-and three-dimensional device simulation modular and extensible. It is a series of tools for simulating processes and gadgets that enable users to carry out and visually assess the result of electrical characteristics (i.e., I_D vs V_G) of devices and simulation-based semiconductors designs. The Atlas framework-based products address the device simulation needs of all analog and digital application areas [36].

ATLAS Inputs and Outputs

In the Atlas simulation, there are two input files. The first one is a text file, which contains ATLAS commands. The structure file is the second, which defines the structure that will be simulated. And also, there are three output files produced in the Atlas simulator. The run-time output is the first output file type, which displays the simulation's progress and shows any problems or warning messages. The log file is the second output type, and it contains or retains

all terminal currents and voltages. The third output file type is the result file, that keeps two-dimensional records of the contents of the solutions variables inside the device for a specific bias point [36].

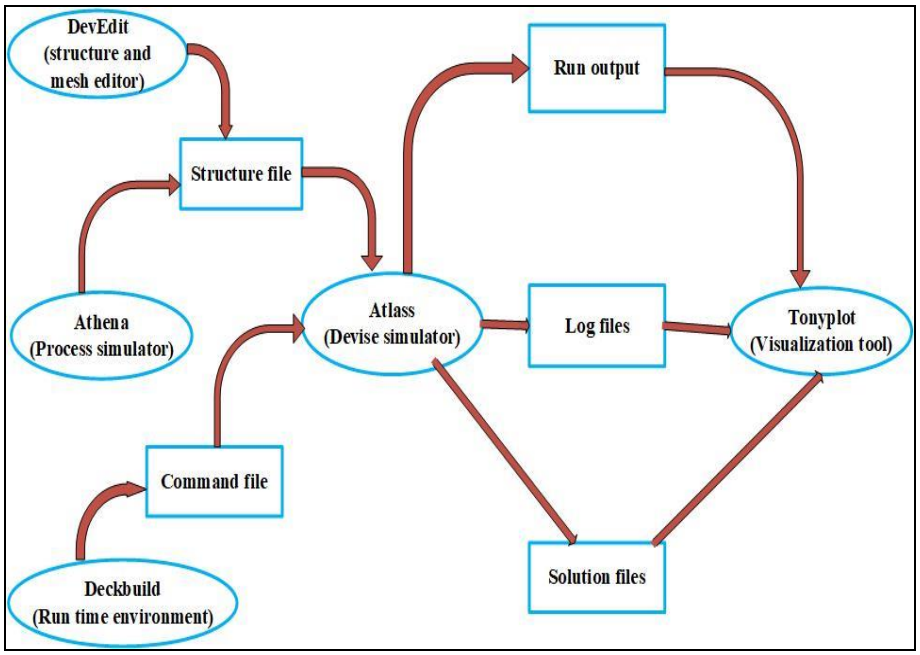

Figure 3.1: Atlas Inputs and outputs files [36]

The ATLAS syntax

A list of commands for Atlas to perform or execute is called an Atlas command file. This list is saved as an ASCII text file, which can be created with DECK BUILD or another editor. Because of its user friendly interface, using the DeckBuild Commands option to prepare an input file is preferable and more accessible [36].

Defining a structure

In Atlas, the structure of the devices can be specified in three methods. The first method is to read an existing structure from a file. ATLAS produces the device structure. The mesh, location, electrode positions, and structural doping are loaded using the MESH statement.

The second option is to use DECK BUILD Automatic Interface tools to transfer the ATHENA or DEVEDIT input structure. The third method uses the Atlas command language to build or create a structure. This study makes or generates all the structures using the ATLAS command language [36].

3.3. Design Methodology

Technology computer-based simulations assess the study of the device performance limits and scaling potentials and solve poor analog/RF parameters performance. Further, the effectiveness of dielectric engineering tunnel FETs, which contributes to the decrement of I_{OFF}, reduction of ambipolarity, and I_{ON} enhancement essential parameter in analog/RF amplification are analyzed.

3.3.1. Simulation flow chart

Different Atlas programming steps are included in this section to simulate and design the structure of DG-TFETs based on device structure, meshing defining, defining a region, doping of region, models, I-V characteristics, parameter extraction, and so on. Furthermore, the DG-TFETs device structure demonstrates using the below flow chart diagram.

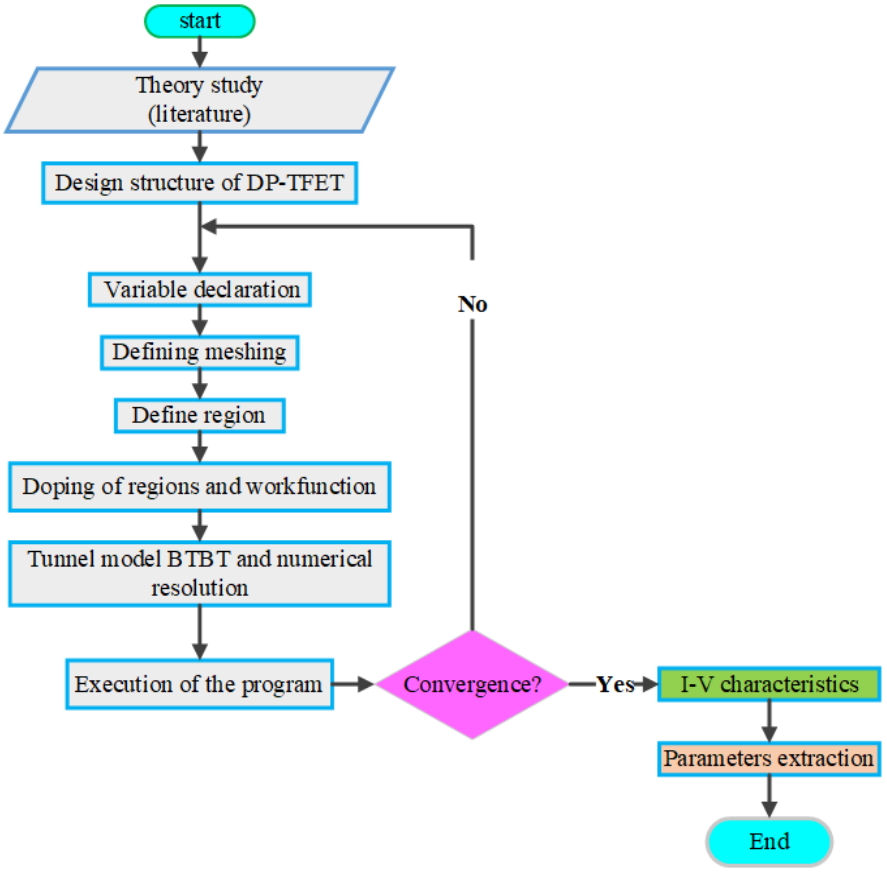

Figure 3.2: Atlas resolution algorithm of DG-TFETs

3.3.2. Simulation Procedures Devices

The device structure of TFETs has been designed in a sequence of defining mesh, region, electrode, doping, and contact.

Meshing

The mesh statement defines the device structure in the 2-dimension Cartesian grid. The x-axis side mesh (X.mesh) occurs on the left to the right hand, and the y-axis mesh (Y.mesh) is from bottom to top [36]. All coordinates or values are entered in microns meter (μm), and the spacing is used to refine the sharpness and precision at a given position [72].

Table 3.1: Atlas Command groups with primary statements in each group

Group	Statements
Structure Specification	Mesh, Region, Electrode, Doping
Material Models Specification	Material, Model, Contact, Interface
Numerical Method Selection	Method
Solution Specification	Log, Solve, Load, Save
Result Analysis	Extract Tony plot

Regions

The region statement separates the initial mesh statement into blocks and defines the initial material parameters, which are then referenced by region number. A region must be assigned to each meshed area of a structure, and the regions must be ordered from lowest to a highest region [36].

Electrode

Once the regions are set, the electrodes must be assigned to the desired region to be electrically analyzed. Any region or section of a region can be allocated electrodes. Gate, source and drain are some of the electrode names used by ATLAS. These parameters were defined using the following statements:

Electrode <location parameters> Name=<electrode name>

The X.min, X.max, Y.min, and Y.max metrics are used to specify the placement parameters in microns. Several electrode statements may have identical electrode names.

It is interesting to note that those with the same electrode name are considered electrically contact [36].

Doping

The doping declaration is the final input needed for the device structure definition. In order to specify how the semiconductor was doped and whether the area is N-type or P-type, additional features might be added (to produce impurity) to the doping statement. [73]. To define doping type parameters, the following statements were used:

Doping <distribution type> <dopant concentration type> <location parameters>

Uniform or Gaussian doping profiles can be found in analytical doping profiles. However, the uniform doping concentration in our study was employed [36].

Material

The physical characteristics and the materials given to the meshes are related via a material statement. The key material properties for the majority of common semiconductors are defined by ATLAS. Because the constructed tunnel junctions depended on silicon semiconductor technology, which is thoroughly researched and recorded, this project effort made full use of the model resources in ATLAS [72].

Simulation Model

The local BTBT model approximates the tunneling barrier and assumes that the lateral electric field is constant throughout the tunneling area. However, a non-local BTBT model considers the electric field change in the tunneling region. Therefore, a non-local dynamic BTBT model to simulate BTBT current in TFET accurately and also, it is used that the Kane BTBT model to find the generation carrier due to band to band tunneling.

Auger and Shockley-Read-Hall recombination model has been added for high impurity atom concentration in the channel region. The energy band-gap is a significant parameter that reduces heavily source region doping at a source-channel junction and increases band-gab with lightly drain doping at the channel-drain junction and directly impacts the tunneling current. Because of this reason, band bap narrowing (BGN) has been added for highly doped sources and lightly doped drains. The Fermi-Dirac model has been used to govern and decreases the charge carrier's concentration. The concentration-dependent mobility model, Lombardi model, and electric-field-dependent mobility model have been used as mobility models, and quantum tunneling direction

models have also been added for the appropriate study of the performance of the TFETs device [74] [36].

After the simulation, a different number of parameters are observed by drawing a cut line along an arbitrary direction specified by two-point in the XY plane. The variation of different parameters, such as electric field (vertical and horizontal electric field direction), electron concentration, and electron BTBT generation, along the direction of the cut-line are examined. Finally, the two-dimensional Silvaco Atlas TCAD simulation justifies parameters by different characteristics [36].

Table 3.2: Description of different models used

Model	Syntax	Comments
Shockley-Read-Hall	SRH	Responsible for generation-recombination, Used for a fixed minority lifetime.
Band Gap Narrowing	BGN	Important in the heavily doped region (Specify band-gap narrowing model).
Lombardi (CVT) model	CVT	To account for the high field mobility effect
Band to band tunneling (Kane)	BBT.KANE	Allows modeling of forward and reverse tunneling
Concentration mobility	CONMOB	They are used for low-field mobility to the impurity concentration.
Auger transition	AUGER	Important at a high current density.
Field dependent mobility	FLDMOB	Used in field mobility.

The statement used in the code is listed below:

Models SRH CVT BGN Fermi Print BBT.Kane print

Output

By default, a structure file contains several values, such as doping, I-V curve, electron concentration, electric field, electron BTBT, etc., by using the output statement [36].

Output val.band con.band u.bbt charge e.lines band.param e.field j.electron j.hole j.conduc j.total ex.field ey.field e.mobility

Solution Specification

The log/solve/save commands are employed in ATLAS simulations to generate data files. Together, these assertions provide data that may be used for different types of analysis. These statements about the relationship between the gate voltage and drain current are utilized in this work to examine device design results [36].

Log

All terminal attributes produced by a solution statement may be recorded to a document using the LOG statement.

Solve

In order to create a result, the SOLVE statement defines which bias factors should be used.

Save

All node point data is saved into an output file using the SAVE statement. For the tunnel junction of the study, the typical use of the LOG/SOLVE/SAVE statements is depicted below:

```
Solve vgate=-2 vstep=0.1 vfinal=2
Save outf=test.str
Tonyplot test.log
Tonyplot test.str
```

3.4 Proposed Double Gate Tunnel FET based biosensors

To fulfill goals, we shall utilize a variety of methods, including reading reviews, data analysis, designing the tubular DG-TFET based structure and finally study and analyzes the proposed work for better biosensor application. In this project work we have utilized the horizontal cross-section of the tubular tunnel FET to perform the electrical characterization. Using the Silvaco TCAD Atlas program, the electrical performance of a Double Gate-Tunnel Field Effect Transistor (DG-TFET) was explored [75]. It gives electrostatic control over the channel via

preventing the drain field line from interfering with the source-to-channel barrier and reducing short channel effects.

3.4.1 Device Structure and Simulation

A. Device Specification

The FET based Biosensors now are the emerging devices for the immobilization of the biomolecules and the major advantage that they are used in label free environment. In this work we are proposing three different device structure with different cavity area and immobilization methods.

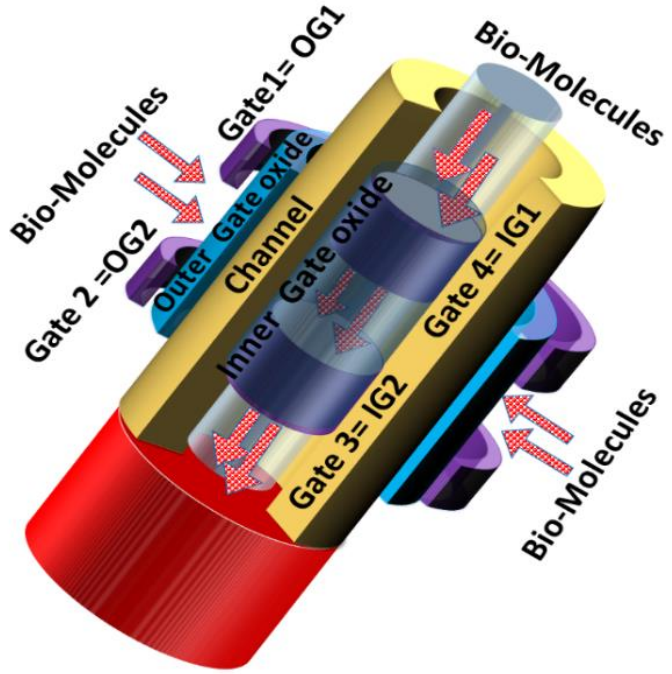

Figure 3.3(a) 3D Structure of Silicon Nanotube Tubular Biosensor

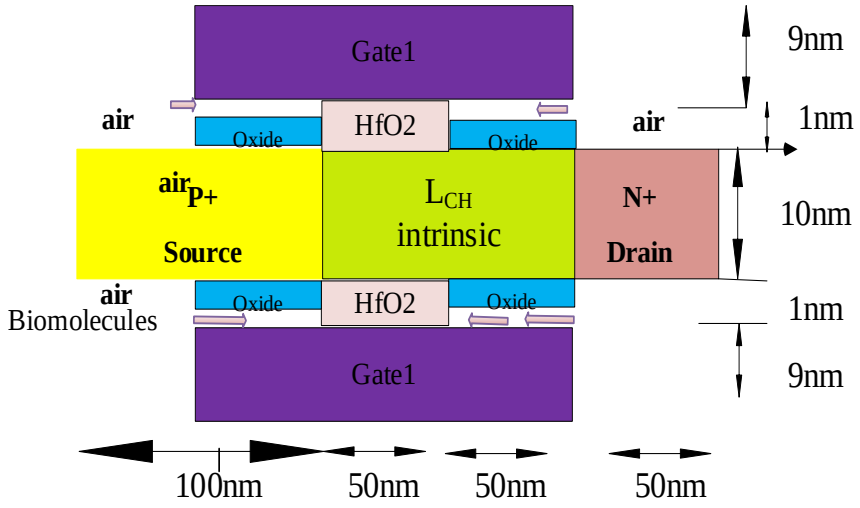

Figure 3.3(b) 2D Structure of DG-BSC-TFET

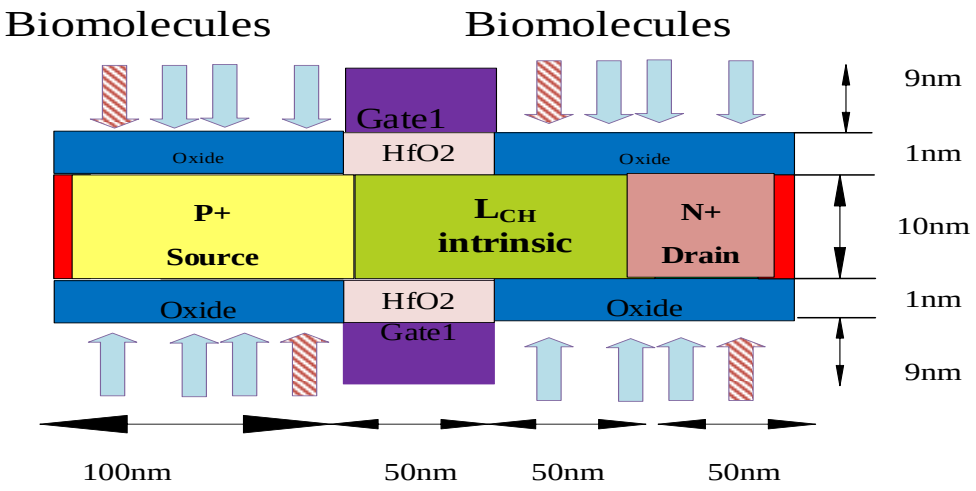

Figure 3.3 (c) 2D structure of DG-FBSC-TFET

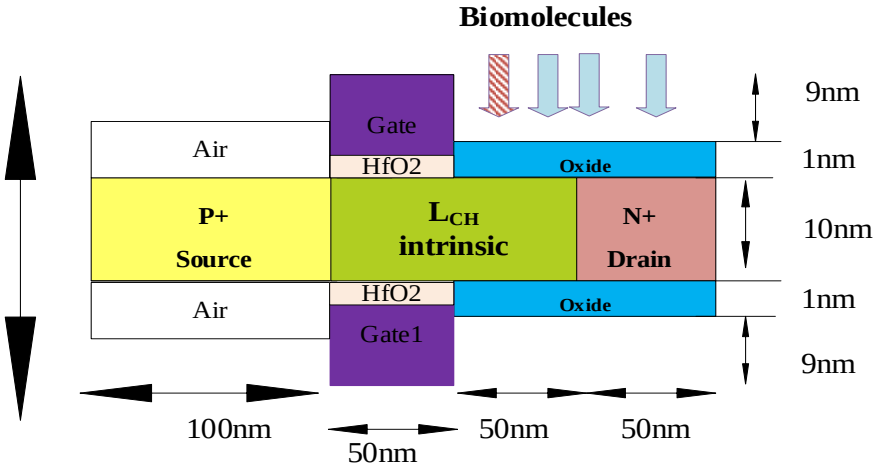

Figure 3.3 (d) 2D Structure of DG-DSC-TFET

In this work the biological molecules are inserted from the top of the device as shown in below Fig 3.3. The Figure 3.3(a) shows the Silicon nanotube tubular biosensor. Because of the shell-core gate stacking arrangement, silicone nanotube FET has already been described in research with a strong electrostatic gate regulation of carriers[10][8]. Here in the proposed structure two gates (inner and outer gate) are designed to control the channel from inside the nanotube and from outside, because of which it is much more efficient than Nanowire FET. Due to less short channel effects (SCEs), in comparison to other designs described in the scientific literature, the silicon Nano tube delivers strong driving current due to its (low DIBL as well as low sub-threshold slope) and substantial volume inversion. In fact, due to a volume inversion, the minority carriers representing the lower energies band as well as the surface charges are responsible for the current flow. For analysis purpose from now onwards we have taken the horizontal cross-section of silicon nanotube TFET and renamed as the double gate TFET (DG-TFET). The first structure we used is the double gate both side cavity Tunnel Field effect transistor (DG_BSC_TFET). In this structure we are using the cavity length of 50 nm in both, source and drain regions and the length of the channel is 50 nm. Metal is used as an electrode, which covers the cavity regions both sides and the gate region. Second structure is defined as the double gate with whole region above the source and drain side are covered with cavity (DG_FBSC_TFET). The metal electrodes are placed in vertical manner, i.e., as parallel to the Y-Axis. The surface to volume ratio is more in this structure because around total 200 nm are exposed for the immobilization of the biomolecules. The last and third structure we have used the double gate TFET with only the cavity at the drain side of 50 nm length and 10 nm of thickness. The gate electrode is covered the cavity as well as the drain region. In this work we are using (DG_DSC_TFET) as the nomenclature for this device structure.

Maximum number of biosensors, however, is dependent on DG-TFET, particularly in which biomolecules are introduced from the both sides of the device structure.

The proposed DG_BSC_TFET structure features a gate length of 50nm, a body thickness (t_{si}) of 9nm, a front and back device oxide thickness (t_{ox}) of 1nm, and a cavity length on both sides i.e., source side and drain side are 100nm. Because the output current is the tunneling current between the source and the drain as controlled by the gate voltage, the Subthreshold slope (SS) value of a TFET is defined by a number of parameters in our proposed work, including gate oxide thickness (t_{ox}), SOI layer thickness, and the steepness of the source doping

profile. The local BTBT models are used to estimate tunneling current from source to drain with fluctuating gate voltage (V_{GS}) [76].

The I_D–V_G graph of DG-TFET has been plotted and observed by using BTBT model which is simulated in the program. The choice of the mesh under atlas is a vital step to have a meeting. Our proposed DG-TFET based biosensor structure are made by fluctuating the typical device and electrical parameters shown in table 3.3 validated by literature [77]. During simulation, different k value biomolecules (k=1, 3, 5, 7 and 9), and in simulation and deliberation, various densities for charged biomolecules are taken into account. The DG-BSC-TFET employed in this research work is shown in Figure 3.3(a, b, c) having three regions: p-type semiconductor by forming source and channel region, and n-type semiconductor forming drain region. Figure 3.3(a, b, c) shows cross section of tubular Structure of DG-BSC-TFET, DG-FBSC-TFET, DG-DSC-TFET with biomolecules immobilized and a cavity length of 100nm each, 200nm each and 50nm respectively. In addition, Lg = 50nm, t_{ox} = 1nm, t_{si} = 9nm; and doping concentration on source, channel, and drain = $1x10^{20}cm^{-3}$, $1x10^{18}$ cm^{-3} and $5x10^{19}$ cm^{-3} respectively are the other parameters considered in this work.

Figure 3.3 illustrates the device design for the Dielectric Modulated Double Gate Tunnel FET (DM-DG-TFET) biosensor employed in this project work. This investigation considers a double gate p-i-n TFET architecture.

The formation of built-in oxide in the Nano-gap cavity regions is considered to be accounted for with a 1nm thick SiO_2 layer. The target biomolecules are induced and fixed in the Nano-gap cavity areas, which serve as detecting sites. In the simulation, a non-local band-to-band tunneling (BTBT) model is used. Inserting dielectric constant material (for instance, streptavidin = 2.1, protein = 2.50, biotin = 2.63, and APTES = 3.57, K>1) into the cavities simulates the entry of biomolecules into the nano-gap cavity (assuming the cavities are entirely filled with biomolecules). To replicate the impact of biomolecule charge, a negative or positive fixed oxide charge (N_F) at the SiO_2 interface is used. Generally speaking, a reference is assumed while figuring out the sensor's sensitivity. As a result, the reference exists when the spaces inside are empty of biomolecules or just when those cavities are stuffed by air. As a result, the following formula is used to characterize the DM-TFET's threshold voltage sensibility, drain current sensitivity, as well as subthreshold slope sensitivity [65].

$$\Delta V_{th} = V_{th(air)} - V_{th(bio)} \text{ ---------- } 3.1$$

$$S_{drain} = \frac{I_{ds(bio)} - I_{ds(air)}}{I_{ds(air)}} \text{ ---------- } 3.2$$

$$S_{ss} = \frac{SS_{air} - SS_{bio}}{SS_{air}} \text{ ---------- } 3.3$$

If the spaces inside have been filled by air, the biosensor's threshold voltage becomes V_{th} (air), whereas if they are filled containing biomolecules, it is V_{th} (bio). In a similar vein when the cavities have been filled with air, these biosensor's on-state drain current and subthreshold swing are represented by I_{ds}(air) and SS_{air}, respectively, whereas when the slots are loaded with biomolecules, they are represented by Ids(bio) and SS_{bio}, respectively. The threshold voltage, on-state drain current, and subthreshold swing are retrieved from the analysis of the DG-TFET's electrical properties to examine the sensitiveness of the biosensor. The three proposed structures are made-up to be used with ATLAS software to examine and analyze the performance of DG-TFET based biosensors. The simulated parameters like sensitivity, ambipolar current, surface potential, charge concentration is studied and analyzed in result and discussion part for biosensor.

Nanogap are incorporated in the oxide layers where the biomolecules are confined in recently described dielectric modulated FET (DM -FET) biosensors. As a result, threshold voltage (V_{th}) and on current (I_{ON}) of the device vary dramatically depending on the dielectric constant and charge behavior of the biomolecules.

A. Simulation Framework

In this project work, the non-local band to band tunneling (BTBT) model is applied for tunneling. In order to investigate the functionality of DG-TFET biosensors clarify it bluntly, this work uses the TCAD toolset to investigate the effectiveness of TFET-based sensors. The proposed DG-BSC-TFET, DG-FBSC-TFET, and DG-DSC-TFET with various high-k materials (HfO_2) are designed with TCAD device simulator called ATLAS Tool. The results are carefully compered and analyzed. For accurate simulation, the relevant models are used. The nonlocal BTBT [78] treats the electric field at every point along the tunneling path as an independent variable, thus the band twisting near the tunneling junction affects the possibility of BTBT

tunneling. The non-local tunneling model is nearer to how TFET simulations actually occurs. As a result, this project work uses the nonlocal BTBT model. Tunneling is a quantum mechanical phenomenon that happens when electrons on the atomic scale have wave-like qualities. When an electron collides with an energy barrier, it can either be reflected or transmitted through.

Table 3.3 Key parameters of this work compared to similar work

Parameters	DM-FGTFET with Si channel (Kanungo et al., 2017)	DM-DGTFET with Si channel (Ahangari, 2017)	DM-EDTFET with Si channel (Venkatesh et al., 2018)	DM-TFET with Si channel (Biosensor et al., 2019)	This Work
Source Length	20nm	30nm	50	20nm	100nm
Drain Length	20nm	20nm	50nm	20nm	50nm
Cavity Length	10nm	10nm	20nm	42nm	50,100nm
Gate length	42nm	35nm	75nm	25nm	50nm
oxide thickness	----	10nm	0.8nm	6nm	1nm
P^+ source doping concentration	$5e19cm^{-3}$	$1x10^{18}$ cm^{-3}	$1x10^{15}cm^{-3}$	$5x10^{19}$ cm^{-3}	$1x10^{20}cm^{-3}$
N^+ drain doping concentration	$5e18cm^{-3}$	$1x10^{19}$ cm^{-3}	---------	$5x10^{18}$	$1x10^{18}cm^{-3}$
Intrinsic doping concentration	$1e12cm^{-3}$	-------	----------	$5x10^{19}$ cm^{-3}	$1x10^{19}cm^{-3}$
Dielectric Materials	SiO_2	TiO_2	SiO_2	HfO_2	HfO_2
Gate work-function (ϕ)	4.8eV	5eV	4.3eV	3.8eV	
Gate voltage	1V	0.7v	1.5v	1.5v	0.2V
Supply voltage (V_D)	1V	1v	0.5v	0.7v	-1V

The height, width, and shape of the barrier determine the likelihood of transmission through or tunneling. Tunneling takes place in the source-channel p^+-i-n^+ junction of n-channel TFETs. Electrons in the p+ source below the source Fermi level may tunnel through the energy gap into

empty states above the Fermi level in the conduction band of the channel with an adequate gate bias. The tunneling current in the non-local band-to-band tunneling model is determined by the band edge profile along the whole path between the tunneled locations. This means that the electric field at each site along the tunneling path changes over time. Tunneling is therefore a non-local process. Figure 3.4 Shows the Quantum tunneling phenomenon at metallurgical junction.

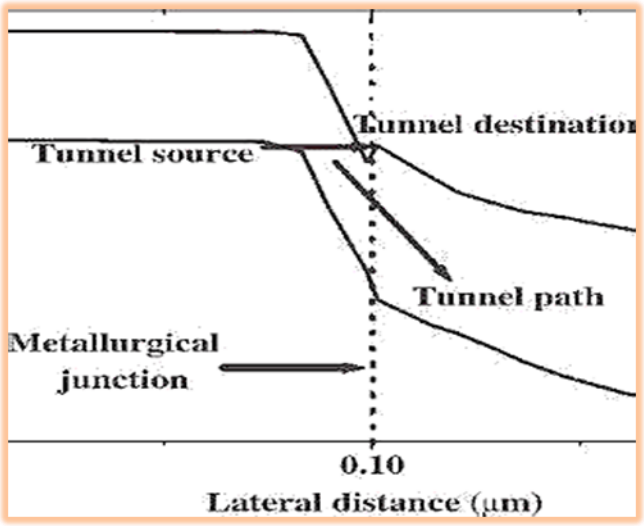

Figure 3.4: Prospective non-local band to band tunneling (BTBT) model *[67]*

The simulator's go atlas command is used to begin the simulation. Further, the double-gate tunnel field effect transistor biosensor must be configured for biosensor applications using appropriate ATLAS instructions such as mesh, region, electrode, doping, and so on. The flow chart shown in Figure 3.2 is the base line to this work and through this step will design and study and analysis the performance of DG-TFET for biosensor application.

Under DG-TFET we study and analyze the proposed work i.e., DG-BSC-TFET, DG-FBSC-TFET, and DG-DSC-TFET based biosensor.

The upstairs project design flow must require the following points:

- The design flow starts with a given set of specification or requirement
- The system should get design with respect to given specification
- At the end, when the desired specifications are not meets, the project has to be modified and re-checked until it meets the required specifications.
- Finally, verification has been done by ATLAS tool software.

3.4.2 Double Gate Tunnel Field Effect Transistor (DG-TFET)

The construction of the DG-TFET is made up of two gates, one at the top called Front Gate and the other at the bottom called Back Gate. Because field lines terminate at the back gate rather than in the channel, electrostatic control of the gate on the channel was improved [79]. Because there are two channels via which current might travel, the ON-current rises. Computer-aided design was used to simulate the performance of the proposed DG-TFET biosensor (ATLAS TOOL). A suitable model is applied in the program to correctly simulate the device parameters. The degree of band bending and the boundary profile have a considerable influence on the amplitude of the tunneling current. The TFET simulation's actual situation is more consistent with the nonlocal tunneling concept.

3.4.3 Design and Simulation Parameters Proposed TFETs Based Biosensors

The parameters used to create the structure in the SILVACO TCAD ATLAS TOOL Software are listed in Table 3.4 below.

Table 3.4 The system implementation parameters

Parameter Name	Symbol	Value	Unit
Source doping	s_d	$1e^{20}$	cm^{-3}
Channel doping	c_d	$1e^{18}$	
Drain doping	d_d	$1e^{19}$	
Source length	s_l	100	nm
Channel length	c_l	100	
Oxide thickness	t_{ox}	10	
Drain length	d_l	50	
Gate length	g_l	50	

3.4.4 Parameters used to simulate a Biosensor Based on DG-TFET

Simulation parameters are a characteristic which are mainly utilized in this work after designing the DG-TFET structure for biosensor applications are:

- ON-current (I_{ON}) to OFF-current (I_{OFF}) ratio
- Ambipolar current sensitivity
- Subthreshold slope (SS) sensitivity

A). Threshold Voltage

The threshold voltage is the smallest potential difference that can be applied between the transistor's gate and source to form a channel. The tangent to the point where the voltage just shoots up exponentially is the threshold voltage as shown in Figure 3.5 The threshold voltage varies depending on the diode's material. The threshold voltage for silicon is around 0.7V, while for germanium it is around 0.3V.

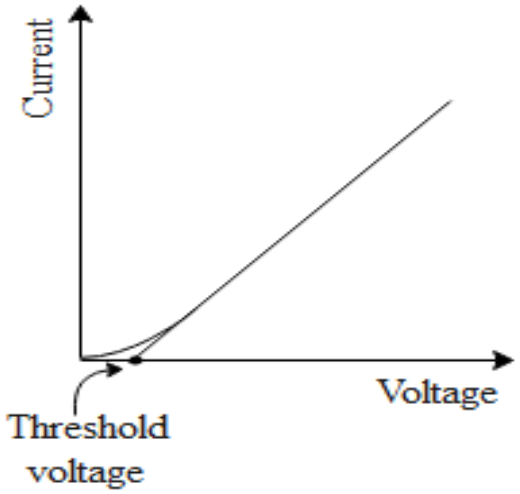

Figure 3.5 Graphical representation of V_{th}

Note: The current increases just slightly before reaching the threshold voltage. This is because the depletion layer is in charge of managing the charge's mobility. Since each semiconductor's depletion layer width is distinct, each semiconductor's threshold voltage is also different.

B). OFF-State Current

The MOSFET is going to be in its OFF state if the voltage at the gate is lower below the threshold voltage. Minority charge carriers across the drain and source cause a current that circulates in the OFF-state, though. Subthreshold current is the name given to this current.

C). ON-State Current

Occurs whenever the MOSFET's gate voltage is higher than its threshold voltage. In this condition, the current flow is referred to as ON current, with the symbol I_{on}. Electrons go from source to drain in a circuit.

D). Subthreshold Slope (SS)

The degree of gate voltage necessary to raise or decrease the subthreshold drain current by a factor of ten is known as the subthreshold swing of a FET and is commonly given in millivolts per decade (mV/dec). The equation 3.4 for subthreshold slop is gives an expression [66],:

$$SS = \frac{nkT}{q} ln10 - - - - - 3.4$$

Here n is a factor which describes the efficiency of the gate voltage in changing the semiconductor surface potential, k is Boltzmann constant, T is temperature in Kelvin and q is electron charge in coulomb. In short channel devices, an appropriate subthreshold slope (60 mV/decade) is essential to minimize the heating effect.

3.5 Proposed Junctionless Tunnel FET based Biosensor (GAA-HJLTF)

The simulated device contains a cavity length of 47nm and 9nm thickness, which allows the structure to immobilize the biomolecules that are coming. The device is varied with respective of different natural biomolecules sensitivity of permittivity values such as urease k=1.64, streptavidin k=2.1, biotin k=2.63, Ferrocytochrom k=4.7,bacteriophage k=6.3,keratin k=8 and gelatin=12 in order to analyses the performance of the proposed devices. The structure of the device is shown in the Figure 3.7. For the representation of the cavity, length, and thickness (width) the symbol used are CV_L and CV_W respectively, where CV_L = 47nm and CV_W=20nm it in both part of the source side. And cavity is the confined space or region within the sensor where the biological or chemical biomolecules interaction takes place. In biosensor, the cavity is engineered to optimize sensitivity and selectivity. In table 3.5, a list of parameters used to design the biosensor device structure is listed. The parameter and the dimensions are the same as figure 3.6. In the biosensor, the cavity region is added in both side and it is open to create a larger space for the biomolecule to immobilize to the device. The length of the whole device became 29nm and the width of the whole device is same 74nm. For the biosensor, the doping concentration is also reduced which is 1e18 cm^{-3}.

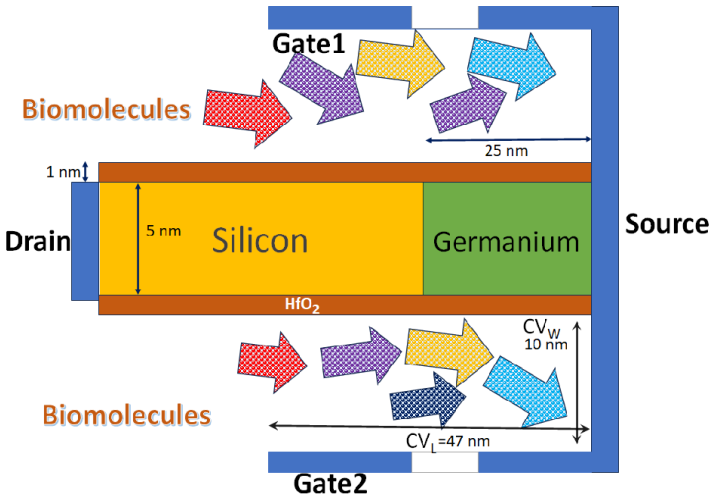

Figure 3.6: Device structure of GAA-HJLTF for biosensor

Table 3.5: List of parameters used for biosensor

Parameter	Values
Channel length and thickness	20nm and 15nm
Gate work function	4.5eV
Source length and thickness	27nm and 5nm
Drain length and thickness	27nm and 5nm
Channel doping	1e18 cm^{-3}
Source doping	1e18 cm^{-3}
Drain doping	1e19 cm^{-3}
Source work function	5.93eV
Dielectric length and thickness	74nm and 2nm
Permittivity of the cavity	K=1.64, 2.63,4.7,63, 8 12
Cavity Length and thickness	47nm and 20nm

3.6 Proposed Gate On Source Based tubular TFET Based Biosensor

Figure 3.7 depicts the silicon nanotube-based tunnel FET biosensor horizontal cross-section. The channel's length is 40 nm, and the tube's width is assumed to be 10 nm. The length of source and the drain are taken as 30 nm each. The source part doping is considered to be of the p type and value is $1x10^{20}$ cm^{-3} and of the drain part it is taken as $5x10^{18}cm^{-3}$. The channel is region is taken just as intrinsic. Hafnium oxide is taken as the gate dielectric with 1 nm

thickness. The hafnium oxide is taken on the channel region as well as 10 nm extended towards the drain region as shown in figure The source region is isolated with the biomolecules using the thin layer of air(k=1). For better immobilization of the biomolecules two different metal i.e., aluminum and tungsten are taken as a gate electrode.

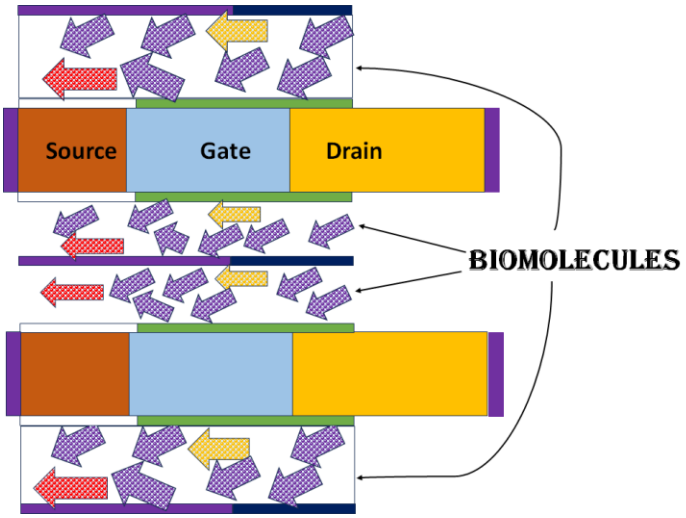

Figure 3.7 Horizontal cross-section of Silicon nanotube tunnel FET based biosensor

Here the gate is overlapping over source region and the cavity region is also increased towards the source region as shown in the figure. Some part of the drain region is also acquired to increase the surface to volume ratio.

The enzymes, bacteria, and other organisms are identified at the inner and outer gate utilizing the dielectric fluctuation, resulting in a change in the sensitivity parameter's value. The drain current is being used in this study as a sensitivity factor. The parameter specifications listed in table 1 are used to approximate the device. By comparing the findings with the databases or previously validated results, it is feasible to determine which categories of biomolecules have come into interaction with a sensor. In this biosensor, the biomolecules can immobilize on the outer and as well as inner surface of gate and source region. The 10 nm of drain region (from .022 µm to .032 µm) is also available for the biomolecules to interact with the surface. A greater number of biomolecules may be detectable inside or outside the tube due to a higher surface to volume ratio. The sensitivity parameter is the drain current. The TCAD oriented 3D device simulator is employed to simulate the operation of the device, and several simulated physics algorithms are included.

In addition to the Shockley Read Hall Recombination Model (SRH), CONMOB, and FLDMOB, we applied the KANE model for band-to-band tunneling process. Regarding numerical iteration, Newton trap model is utilized.

Table 3.6 Device Specification for Gate on source TFET

Parameter	**Value**
Channel length	40 nm
Tube diameter	10 nm
Source/drain length	30 nm
Oxide thickness	1 nm
Source doping	1×10^{20} P type
Drain doping	1×10^{18} /cm^3
Gate oxide material	HfO_2
Dielectric constant (k) modulation range	K=1 to K=9

CHAPTER FOUR
RESULTS AND DISCUSSION

FET-based biosensors are more gaining attention today due to their small sizes, label-free detection, easy manufacturing process and well-established physics behind [22].Biosensors are the analytical device which transmits a biological response into the processable and quantifiable signal. There are two types of methods which are generally used to detect the presence of biomolecules: dielectric modulation and gating effect. In gating effect-based biosensors the dielectric material of the gate is interchanged by a thin layer of receptors which is fused with the charged biomolecules. A subsequent change in the energy band of the device is recorded and hence, the change in drain current is also noted[12]. In dielectric modulated biosensor some part of the gate material is etched out so as to form a nanogap. When the neutral or charged biomolecules sit into the gap, it causes a change in the dielectric constant of the gate. Thus, all the capacitances associated with the gate terminal is varied due to which the drain current either increases or decreases depending on the type of biomolecules entered into the nanogap [60].

Simulation is a realistic and systematic method of evaluating a complex system. In this study, the Dielectric Modulated horizontal cross section of tubular tunnel FET have been considered as per the methodology section [Chapter 3]. The DG-BSC-TFET, DG-FBSC-TFET, and DG-DSC-TFET for biosensor application are examined via simulation using the ATLAS tool. Further the heterojunction Junction-less tunnel FET (GAA-HJLTF) based biosensor is investigated as an application of biosensor. Finally, the gate on source based tubular tunnel FET is studied and utilize for the functioning of detecting microorganism. In this project work, the simulations are used to estimate the electrical characteristics of the biosensors, such as ON-Current, ON current-to-OFF current ratios, electric field, electron concentration and other parameters including sensitivity. Finally, all the parameters are analyzing and observed to conclude this work. In this chapter results of biosensing FET based devices are discussed.

4.1 Analysis of DG_BSC_TFET

The ON-state energy band diagram of DG-BSC-TFET biosensor is depicted in Figure 4.1(a). As it is observing from the figure the tunneling gap between the channel and the drain junction is decreased due to the negative gate voltage (V_g=-1v) application at the gate terminal to study the ambipolar behavior of the device.

In Figure 4.1 (b), the OFF-state energy band diagram of DG-BSC-TFET is given. The device is not in conduction because the applied gate voltage is 0V. In the ON-State because of the existence of biomolecules in the gap region, the Tunneling width between channel and drain junction is minimal, and electrons require little energy to move from the Valence band (VB) of the channel to the conduction band (CB) of the drain region.

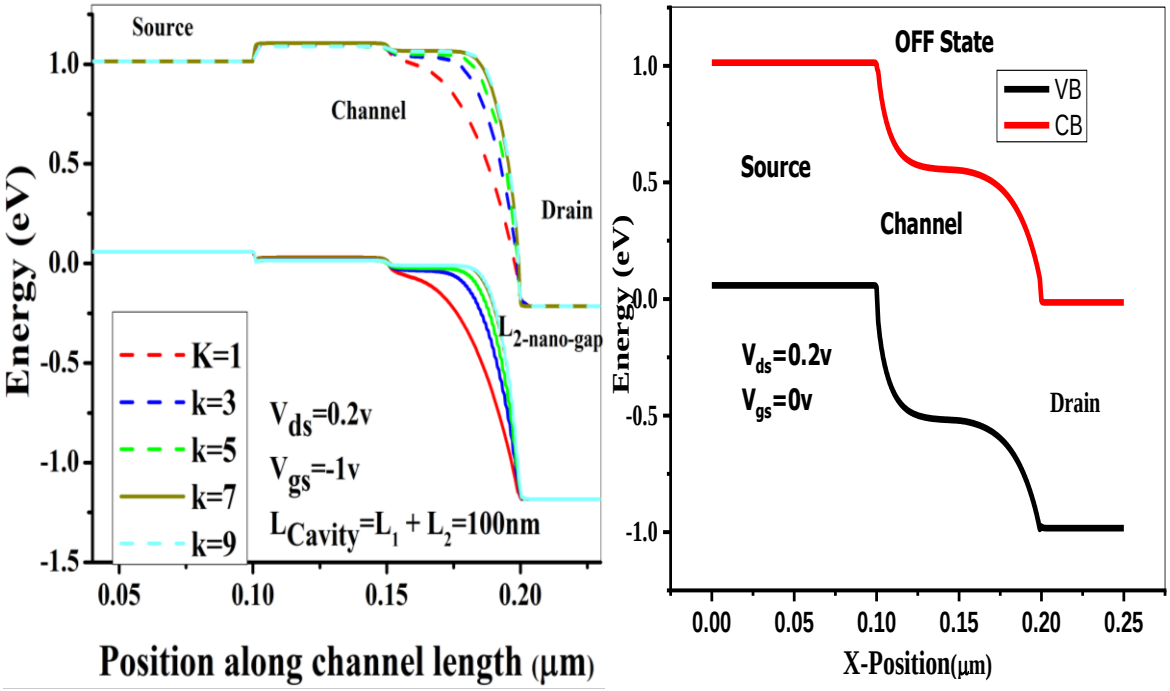

(a) (b)

Figure 4.1 (a), (b) DG-BSC-TFET biosensor energy band diagrams with ON and OFF states at V_G=-1V, V_D=0.2V and V_G=-1V, V_D=0V, respectively.

As the dielectric constant of the biomolecule is increasing, means k of the cavity gap is increasing than the tunneling gap is decreasing therefore, the probability of the tunneling is increased. In this work we have used five dielectric constant values to realize with the practical environment, here we used k=1, k=3, k=5, k=7 and k=9. We have done all the simulations using V_D=0.2V. As we have seen when the K value increases the tunneling gap between the channel drain interface decreases, due to which the ambipolar current is increased.

The figure 4.2 presents the output characteristics of DG-BSC-TFET as a function of gate bias with different dielectric constant varying from k=1 to k=9 at V_{DS} =0.2V. From the graph we observe that the presence of neutral biomolecules with k varying has an effect on the transfer characteristics and a significant variation in ambipolar conduction.

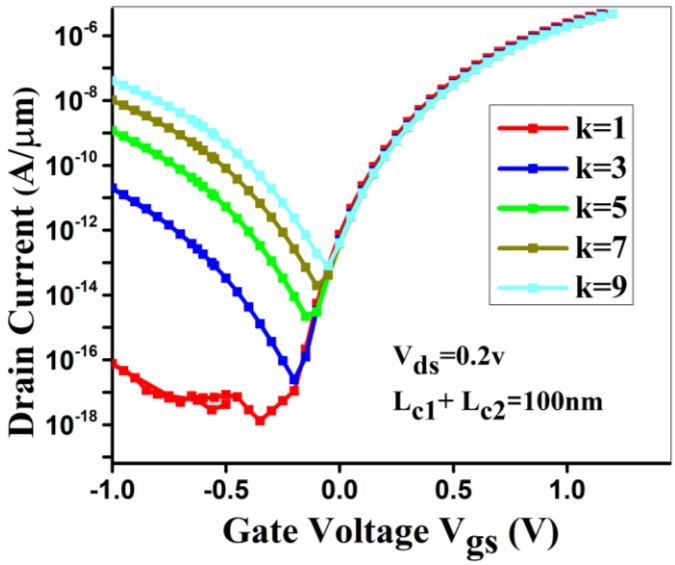

Figure 4.2 Transfer characteristics of DG-BSC-TFET with different dielectric constant (k).

When the dielectric constant (k) increases the major variation is noted in the ambipolar current and the leakage of the current. As shown in Figure 4.2 the ambipolar current is increased on filling the gap with high k biomolecules. The value of ambipolar current for k=3 at neutral charge is $3.56x10^{-11}$ A/μm for DG_BSC_TFET.

However, it has the unique attribute of am-bipolarity, which allows current to flow for both high negative and positive gate voltages. Because of the TFET's ambipolar conduction, it is less successful in complementary circuit applications, limiting its use in digital circuit design. Figures 4.3 (a) and (b) show the effect the presence of charged biomolecules like DNA, **nucleoside triphosphate (negatively charged) and polyamine (positively charged), etc.,** on the transfer characteristics. In this work absence of biomolecules in the gap region are realizing with air (k=1) and the figure is drawn for 10 different charge values from $-1x10^{11}$ cm^{-3} to $5x10^{11}$ cm^{-3} . To ease the simulation process the value of k is kept at 5.

It is observing in the figure on increasing the biomolecule charge value there is no change in the drain current but the ambipolar current is decreasing. When the negative charged biomolecules are present in the cavity region, the on-current is approximately fixed $5.17x10^{-6}$A/μm, and there is no any significant change when the positive charged biomolecule are present in the cavity region, for positive charged biomolecules the value of ON-Current is $5.76x10^{-6}$A/μm. It can be observed from the graph on increasing the value of charged

biomolecules in the cavity region the ambipolar current is decreasing at charge $5x10^{11}$ the I_A is $1.6x10^{-9}$ A/µm and for charge $-5x10^{11}$ I_A is $2.3x10^{-8}$ A/µm.

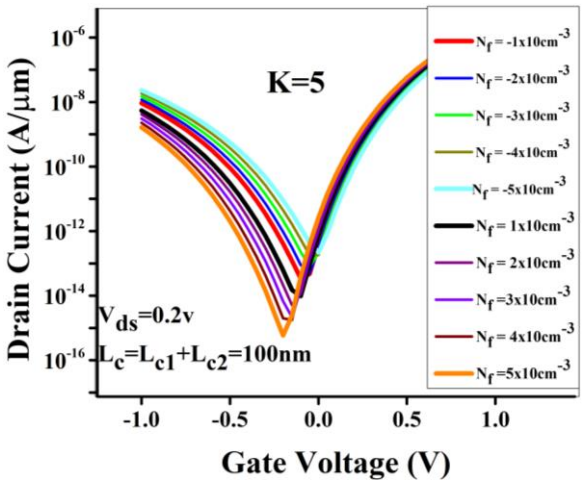

Figure 4.3 Impact of Positive charge and negative Charge biomolecules on transfer characteristics of DG_BSC_TFET at k=5.

Figure 4.4 illustrates how the electric field of a DG-BSC-TFET biosensor changes when the dielectric constant for a biomolecule varies along the x-position. Because biomolecules' dielectric constant increases, it is apparent that the vertical electric field intensity is decreasing. While on the horizontal electric field for cavity length of 100 nm on both sides the electric filed is increase when, high k biomolecules filling in the gap.

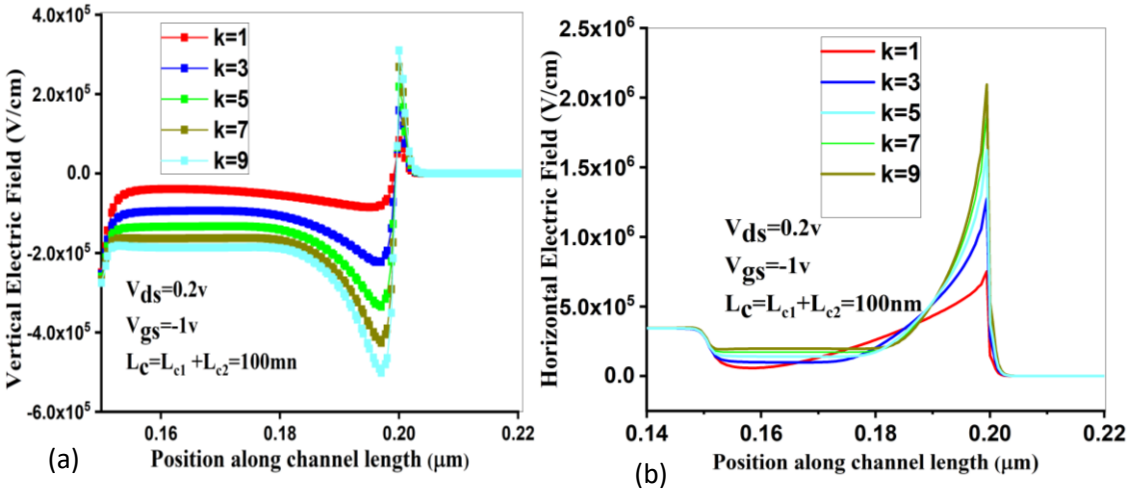

Figure 4.4 (a) Vertical Electric Field (b) Horizontal Electric Field along, x axis for DG-BSC-TFET

Figure 4.4 (a) depicts the variation in the vertical electric field of a DG-BSC-TFET biosensor with varying dielectric strength and Figure 4(b) shows the variation of horizontal

electric field with reference to channel length. Because of the increased dielectric constant of biomolecules, the electric field characteristics show a considerable decrease on vertical and horizontal position along channel length. The tunnel barrier width under the nanogap cavity grows when the value of dielectric constant are altered in the cavity region increases due to a smaller electric field, resulting in a decrease in tunneling electrons from the channel to drain region. When the charge density of the biomolecule is reduced, the on-current to off-current ratio of the DG-BSC-TFET based biosensor is also increased. When cavities are created on the source and drain sides but no biomolecules are present inside the cavity, the cavity gap region is filled with air, resulting in minimum field strength under the cavity in the case of horizontal electric field. When neutral biomolecules with k>1 are present in the cavities, the smaller surface potential rises result in the variation in the electric field which helps in detecting the particular type of biomolecule. Figure 4.5, shows the sensitivity graph for different dielectric constants. Here we have taken the ambipolar current as the sensitivity parameter.

The sensitivity is calculated as the ratio between ambipolar current (I_A) at K=x and the (I_A) at K=1.

As shown in the Figure. 4.5 a considerable increase in the sensitivity is noticed when the dielectric constants of biomolecules are increasing. Sensitivity of DG-BSC-TFET is approximately increases linearly as dielectric constant of the biomolecule increase and it shows good improvement in the field of biosensor.

For all three structures, the sensitivity is expressed as [78]:

$$\text{Sensitivity} = \frac{\text{Ambipolar current (k = x)} - \text{Ambipolar current (k = 1)}}{\text{Ambipolar current (k = 1)}} - - - -4.1$$

Where, K is dielectric constant (1, 3, 5, 7, and 9). Figure 4.5 demonstrates the biosensor's sensitivity, it is described as the difference in ambipolar current between conditions with and without biomolecules. When immobilized biomolecules cause the effective dielectric constant of the nano-gap to increase, sensitivity increases and it is illustrated in the sensitivity graph.

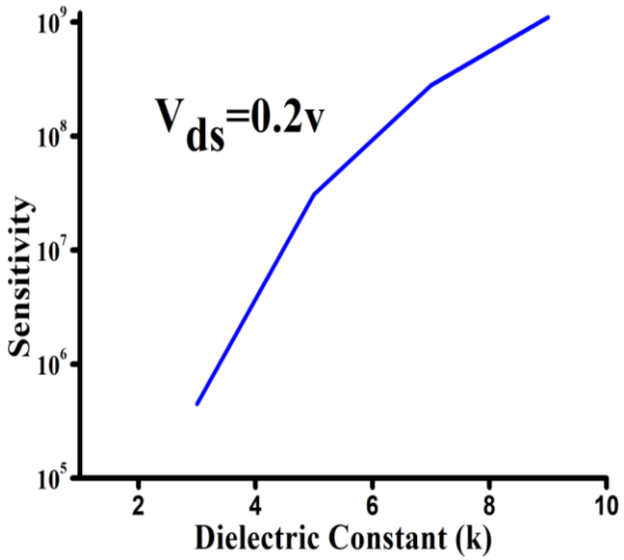

Figure 4.5 Sensitivity of DG-BSC-TFET at V_{GS}=-1V and V_{DS} =0.2V

4.2. Analysis for DG-DSC-TFET

The energy band diagram for double gate drains side cavity- tunnel field effect transistor with cavity length 50nm is shown on fig.4.6. Findings display that in the overlapping gate-on-drain TFET structure, variations in the dielectric constant have a greater impact on the ambipolar current than variations in the charge density of the biomolecules in the nano-gap.

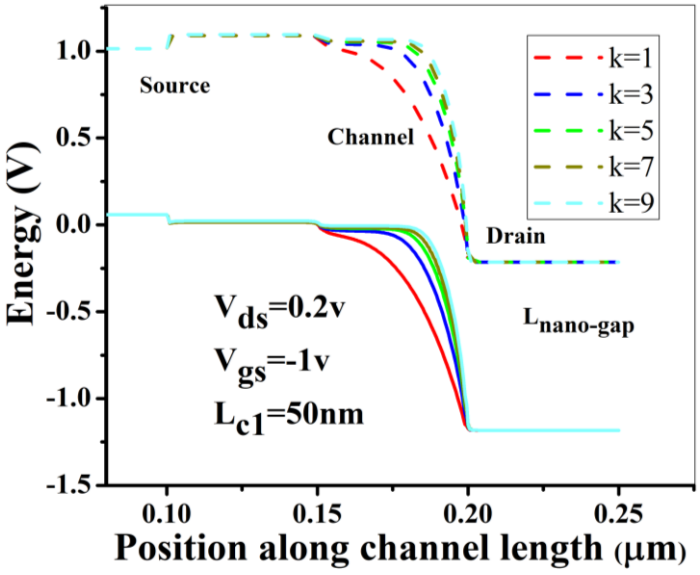

Figure 4.6 DG-DSC-TFET biosensor energy band diagram

As a result, the overlapping gate-on-drain TFET may effectively be employed for the detection of immobilized biomolecules by monitoring variations in the ambipolar current brought on by the value of the dielectric constant as well as the charge inside the biomolecules.

In accordance with the fact that different biomolecules have varied dielectric constants, a real detecting event of the attached biomolecules within the nano-gap was mimicked by changing the dielectric value of a nano-gap [17].

Figure 4.7(a) shows the dielectric strength of biomolecules without charge interference (i.e. charge neutral) increases, the ON-current increases while the ambipolar current increases of current is decreasing at 0v. The dielectric constant k=3 is shown to be the optimal value for this graph, with low ambipolar current and same ON-current values of $1.43x10^{-10}$A/μm and $8.7x10^{-6}$ A/μm, respectively. Form this observed that as dielectric constant of the biomolecule is increase for neutral charge, there is significant change on ratio of I_{ON}/I_{OFF} of $1.5x10^{10}$A/μm. Figure 4.7(b) presents the impact of charged biomolecules on the transfer characteristics of DG_DSC_TFET. There is a no change in the drain current but the ambipolar current is varying when the charged biomolecules are embedded into the cavity region. On increasing the charge value, the I_A is decreasing, so by this mechanism we can able to distinguish between different types of biomolecules.

The major cause in a reduction in I_A due to a decrease in electric field with an increase in negative charge density.

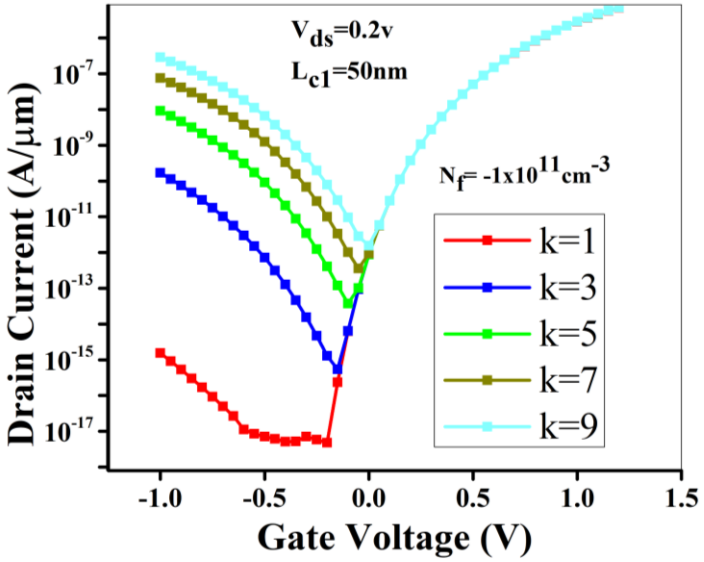

(a)

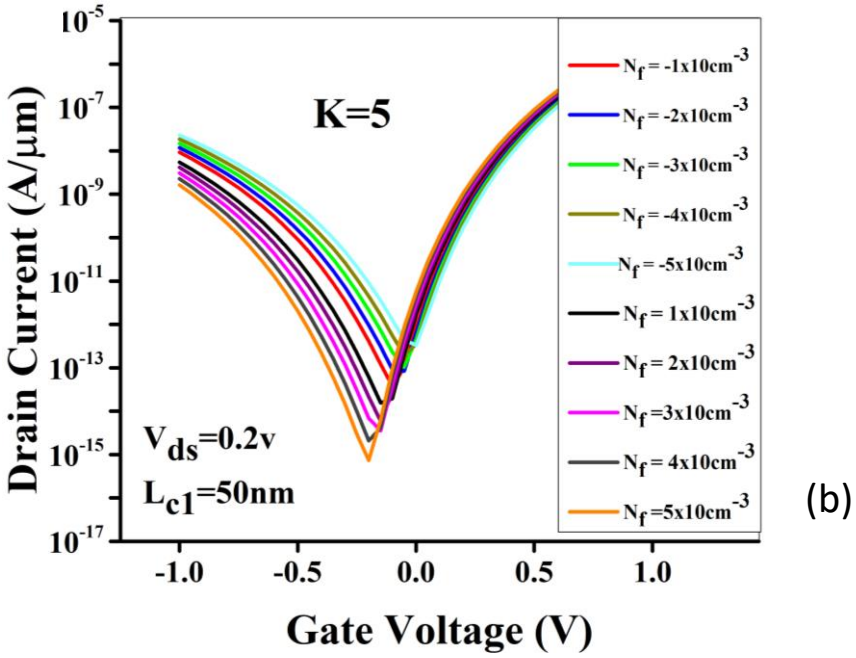

Figure 4.7 (a) Effect of Dielectric Constant, k (b) and Impact of Positive charge and negative Charge biomolecules, on transfer characteristics of DG_DSC_TFET at k=5.

The major cause is a decrement in I_A due to rise in electric field with an increase in negative charge density. Similarly, when positive charge density increases the drain current sensitivity is increasing as seen on Figure 4.9 (a). The positive charge density has great effect on the transfer characteristic of DM-TFET based biosensor.

Figure 4.8 (a) and (b) demonstrates the electric field along the channel's length without and with biomolecules with neutral charge and different dielectric constant k. The charge carriers are electrons or hole, which flow from source to drain through an active channel. This flow electron from source to drain is controlled by the voltage applied across the gate and source terminal. At the tunnel junction, there is a drop in the electric field, which controls the possibility of tunneling and the pace at which BTBT is generated. Thus, the electric field has an exponential relationship with the generating rate. When the electric field increases, the rate of generation rises and I_A decreases. Hence Electric Field is another important parameter to be considered. Because of a boost in the dielectric constant for biomolecules, it has been seen that the electric field properties have significantly changed. Figure 4.8 (a) and (b) describes the variation in the electric field of a DG-DSC-TFET device structure which is proposed as the biosensor. Because of the increased dielectric constant of biomolecules, the electric field characteristics show a considerable increase.

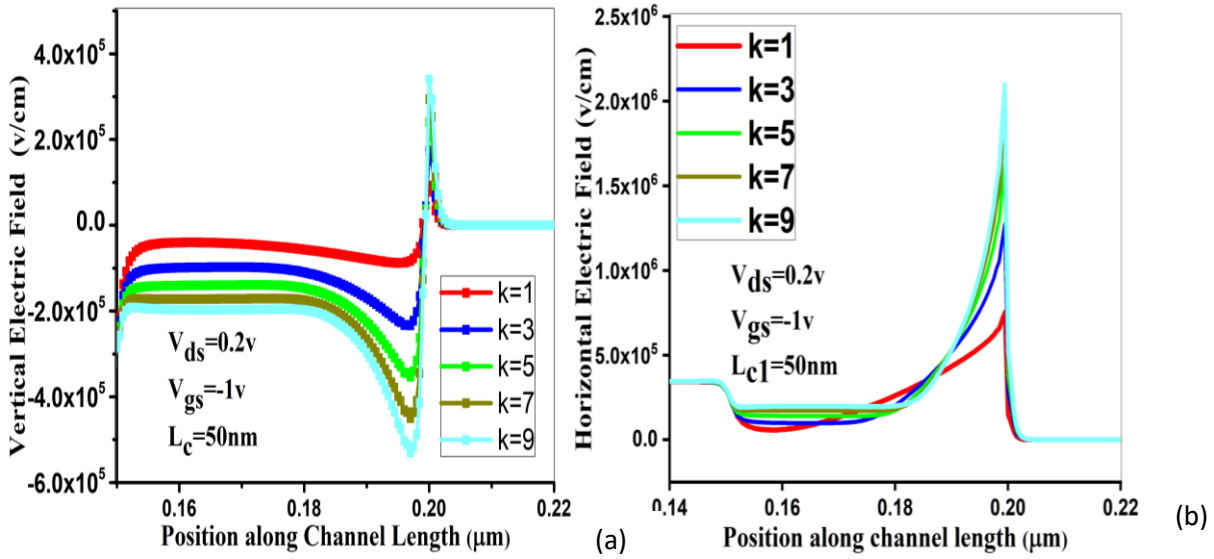

Figure 4.8 (a) Vertical Electric Field (b) Horizontal Electric Field along, x axis for DG-DSC-TFET

Although the charge density is not considered in the Figure 4.8 but it is shown from the Figure 4.7 (b) the tunnel barrier width under the nanogap cavity grows when the negative charge density in the cavity region increases due to a smaller electric field, resulting in a decrease in tunneling electrons from the source to the channel region.

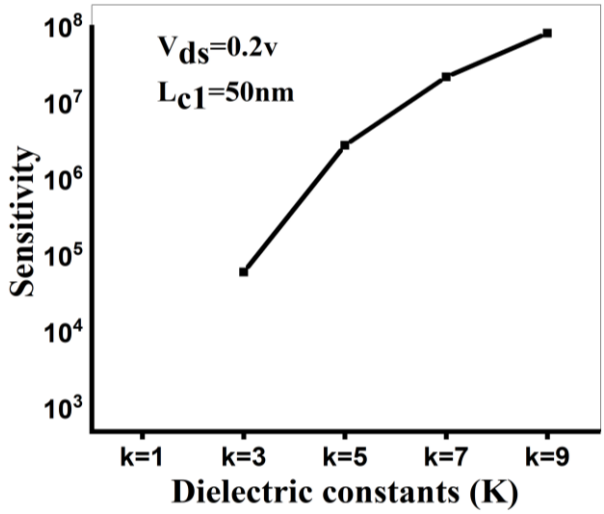

Figure 4.9 Sensitivity of DG-DSC-TFET at V_{GS}=-1V and V_{DS} =0.2V

The sensitivity is calculated as the ratio between ambipolar current (I_A) at k=x and the (I_A) at k=1. As shown on the Figure 4.9, a considerable increase the sensitivity is noted when the dielectric constants of biomolecules are growing. Sensitivity of DG-DSC-TFET is approximately

increases linearly as dielectric constant of the biomolecule increase and it shows good improvement in the field of biosensor.

4.3. Analysis for DG-FBSC-TFET

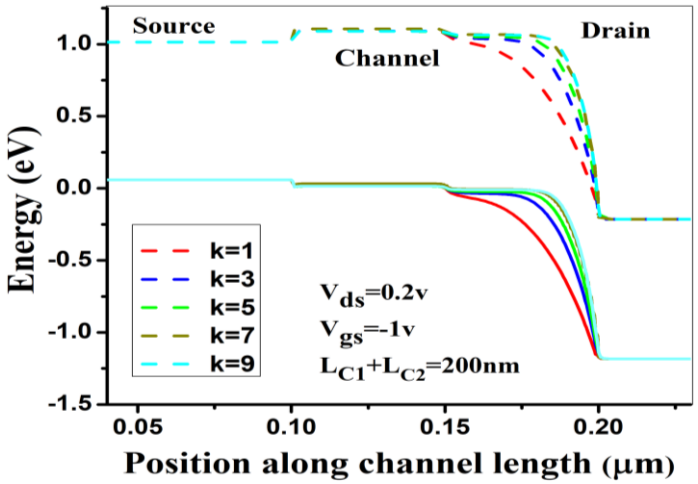

Figure 4.10 Energy-band profiles of conventional double gate full both side cavity-tunnel field effect transistors (DG-FBSC-TFEF)

The energy band diagram for double gate-FBSC-TFET based biosensor shown on Figure 4.10. As we have seen in the above graph on increasing the dielectric constant the tunneling barrier is decreased. The band diagram is made at V_{gs}=-1V and V_{ds}=0.2V due to which the source channel junction tunneling not possible.

The orientation of low-k biomolecules boosts or lowers the sensitivity of dielectric modulation-based biosensors, depending on whether the material is n-type or p-type under the nanogap applied to immobilize the biomolecules [80]. We have seen on the graph that, ambipolar current varying (I_A) improves dramatically on both charged biomolecules as the dielectric constant rises from unity to a larger value seen on Figure 4.11. As the positive charge density increases, the ambipolar current decreases. From Figure 4.11 (a) graph low ambipolar current is Occurred at k=3 for neutral biomolecules. From figure 4.11(b), we found that for DG_FBSC_TFET as charged biomolecules immobilization increases the ambipolar current is decreasing on increasing the charge value.

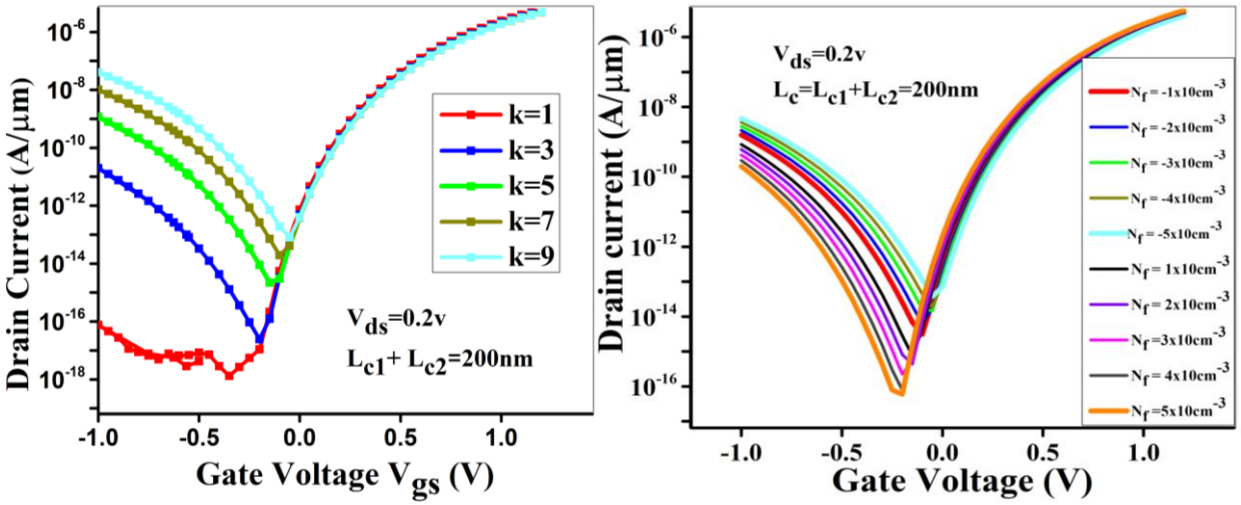

(a) (b)

Figure 4.11 (a) Effect of Dielectric Constant, k (b) Impact of Positive charge and negative Charge biomolecules, on transfer characteristics of DG_FBSC_TFET at k=5.

The ratio between the ambipolar current (I_A) at k=x and the (I_A) at k=1 is used to compute the sensitivity. When the dielectric constants of biomolecules increase, as illustrated in the graph below, the sensitivity increases significantly. The sensitivity of the DG-FBSC-TFET rises approximately linearly as the dielectric constant of the biomolecule increases, indicating a significant advancement in the field of biosensors.

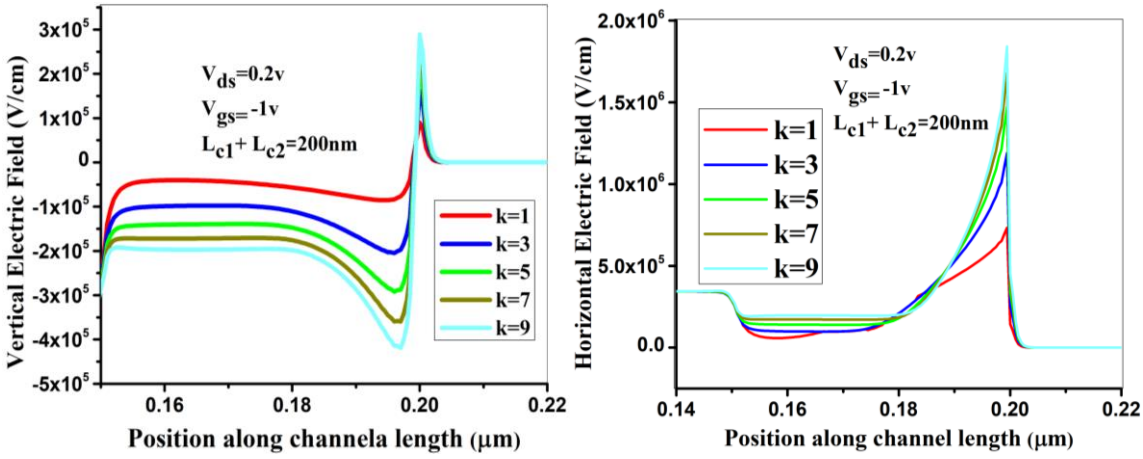

Figure 4.12 (a) Vertical Electric Field (b) Horizontal Electric Field along, x axis for DG-FBSC-TFET

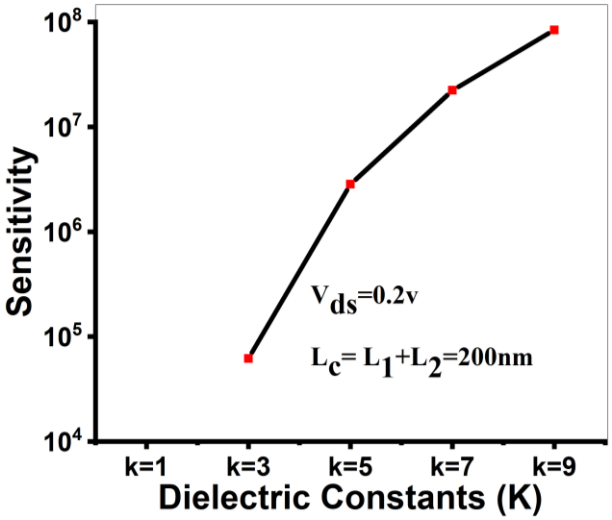

Figure 4.12 Sensitivity of DG-FBSC-TFET at V_{GS}=-1V and V_{DS} =0.2V

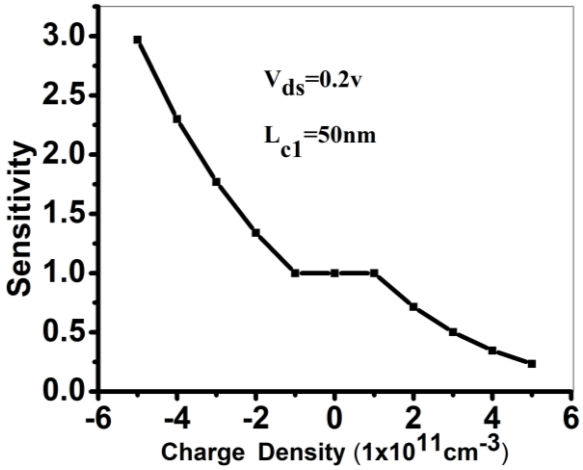

Figure 4.13 Sensitivity (charge) versus Charge Density for DG_FBSC_TFET

We have calculated the sensitivity related to the charge density for DG_FBSC_TFET and it is illustrated in Figure 4.13. In this graph it is observed that when we are increasing the charge density values vary from -5 $x10^{11}$ cm^{-3} to 5 $x10^{11}cm^{-3}$ the related sensitivity is decreasing.

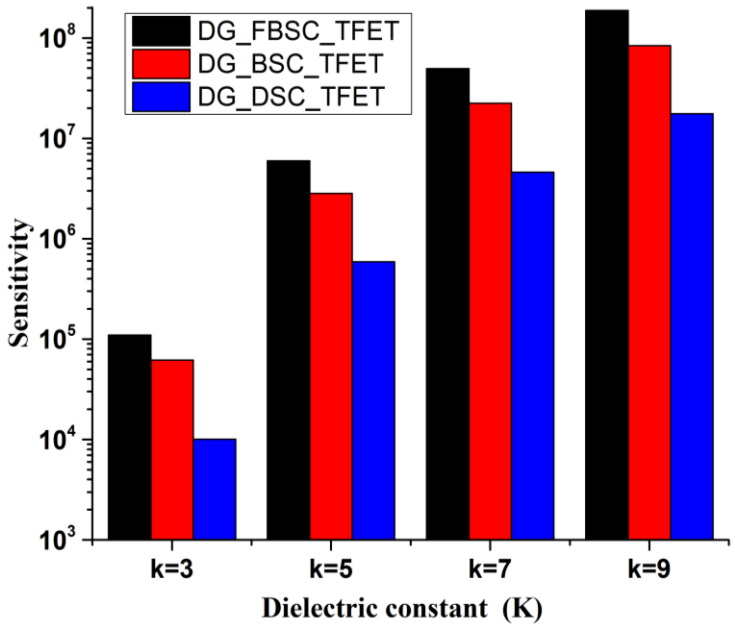

Figure 4.14 Sensitivity Comparison between three proposed structures i.e., DG_BSC_TFET, DG_DSC_TFET and DG_FBSC_TFET

Out of them one is sensitivity, as we have already defined that we are using the ambipolar current as the sensitivity parameter and in Figure 4.14 the comparison between the three proposed structures are given in the form of bar diagram. Out of them three structures the sensitivity of DG_FBSC_TFET is best for all the neutral biomolecules. This is due to the fact that volume to surface ratio in this structure is more compare to the other structures. For K=5 the Sensitivity of FBSC structure is 100 times (10^2) more than DSC structure. Table 4.1 shows the impact of charged biomolecules immobilization in the cavity region on the ambipolar current ,sensitivity of the biosensor and the ON-current to OFF-current ratio for the three proposed structures which we have discussed in the previous chapters . The table specified the biomolecule which have charge densities N_f=-1x10^{11} cm^{-3} and N_f=1x10^{11} cm^{-3} for the varying k values. As shown in table the sensitivity increases as the effective dielectric constant of the nano-gap increase due to the presence of the biomolecules.

From the tubular comparison among three proposed structures for biosensor application, the DG-FBSC-TFET found to be better option. DG-FBSC-TFET also shows better sensitivity and improved ambipolar current when compared with both DG-BSC-TFET and DG-DSC-TFET for biosensor application. The major advantage in the DG_FBSC_TFET structure is it has more

volume to surface area due to which the more area comes into contact of the neutral ad charged biomolecules.

Table 4.1 Optimization of electrical parameters determined for our planned DG-TFET work

S.No.	Parameters	DG-FBSC-TFET	DG-BSC-TFET	DG-DSC-TFET	
		K=5, N_f = -1x$10^{11}$$cm^{-3}$			
1	I_{ON}	6.204x10^{-6}	4.28x10^{-6}	5.85x10^{-6}	A/μm
2	I_{OFF}	2.98x10^{-14}	2.5916x10^{-14}	3.97x10^{-14}	
3	I_{ON}/I_{OFF}	2.0818x10^{8}	1.6514x10^{8}	0.717x10^{8}	
4	Ambipolar current (I_{amb})	1.69x10^{-9}	8.049x10^{-9}	9.38x10^{-9}	
5	K=5, N_f = 1x$10^{11}$$cm^{-3}$				
6	I_{ON}	7.27x10^{-6}	8.47x10^{-6}	7.70x10^{-6}	A/μm
7	I_{OFF}	6.739x10^{-16}	9.612x10^{-16}	9.98x10^{-16}	
	I_{ON}/I_{OFF}	1.078x10^{10}	0.88x10^{10}	0.715x10^{10}	
8	Ambipolar current (I_{amb})	1.60x10^{-9}	1.9117x10^{-9}	2.026x10^{-9}	

The simulated structural design result is evaluated using the Silvaco Atlas TCAD simulator. Firstly, the graphical comparison of conventional JLTFET and proposed GAA-H-JLNTFET has been presented. The simulated transfer characteristics (I_D-V_G) and other device characteristics parameters i.e., Electron BTBT generation rate, Energy band diagram, Electric field along X axis, and electron concentration of GAA-H-JLNTFET is studied and analyzed their impact on the low power characteristics of the device. Further the proposed device is utilized as label free dielectric modulated low power biosensor. In dielectric modulated biosensor we are realizing different type of biomolecules by varying their unique dielectric constant values. To prove the applicability of the biosensor the sensitivity of the biosensor is also calculated. Here we have taken the drain current as the sensitivity parameter. The value of the drain current is varying when different types of biomolecules are immobilized inside the cavity region.

4.4 Analysis of GAA-H-JLNFET as a Biosensor

This section discusses the biosensor application implemented on the proposed GAA-H-JLNTFET after a cavity is inserted to mobilize the biomolecules. Generally, there are two types of biosensing techniques which are used by most of the researcher i.e., one is gating technique and the other is dielectric modulated technique. In this work we have utilized the dielectric modulated based techniques to implement the simulated biosensor using the junction less Tunneling device. The biomolecule that are used are neutral biomolecules (without any charge). In addition, their permittivity is varied as per the biomolecules mentioned in the Table 4.2.

Table 4.2 Biomolecules and their dielectric constant value

Biomolecules	K value
UREASE	1.64
BIOTIN	k=2.64
FERROCYTOCHROM	4.7
BACTERIOPHAGE	6.3
KERATIN	8
GELATIN	12

Figure 4.15 shows the drain current variation when the permittivity is varied for different types of biomolecules (as shown in table) and as the permittivity of the cavity is increasing the drain current is increasing. In biosensor the permittivity of the cavity or the sensing region or active region affect the sensitivity of the device since permittivity determines the sensing of capacitance structure, which is typically influenced by the presence of biomolecules.in this work the cavity width is taken as 10 nm upper and 10 nm lower and the length of the cavity is taken as 47 nm. If the Volume to surface ratio is more the greater number of biomolecules can possible to immobilize with the surface and the better prediction for the disease is possible. The capacitance varies as the permittivity of the cavity is increasing due to interaction with the biomolecules.

This variation of the capacitance noticed in the variation of drain current. In figure 4.15 at k=12 shows high ON current. The effect of electric field and permittivity of the cavity are directly proportional when the permittivity is increasing the electric filed is also keep on increasing the relation can be given by

$$E \propto V/(\epsilon * d) \text{- - - - - - - - - -} 4.2$$

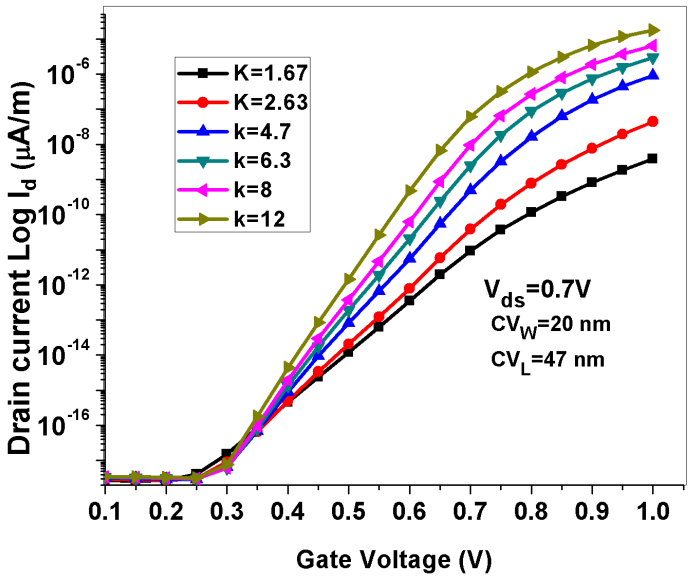

Figure 4.15: **Variation of drain current with immobilization of different biomolecules**

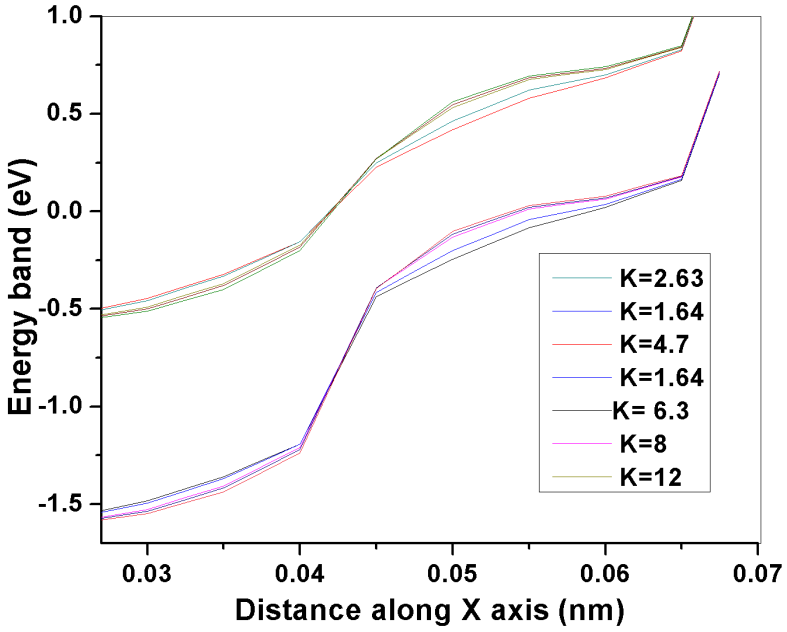

Figure 4.16: **Energy Band Diagram with respect to different biomolecules**

In the biosensor the energy band diagram illustrates the distribution of energy level within that material structure, including the CB and VB. The variation of the permittivity of the biosensor impacts the energy band diagram and subsequently affect the device performance, in Figure 4.16 shows the energy band diagram for the neutral biomolecules. When the permittivity is increasing it alters the electric field distribution and potential profiles in the device. This in return affects the energy band diagram and modifies the shape as the conduction band an upward

shift and Valance band downward shifts. Figure 4.17 (a) and (b) show the impact of immobilization of different types of biomolecules on the total current density and electron concentration, respectively. Form the Figure 4.17 it is observable that increasing the value of dielectric constant, the total current density and electron concentration both are increasing. Changes in permittivity can modulate the capacitance, leading to variation in electron concentration and current density.

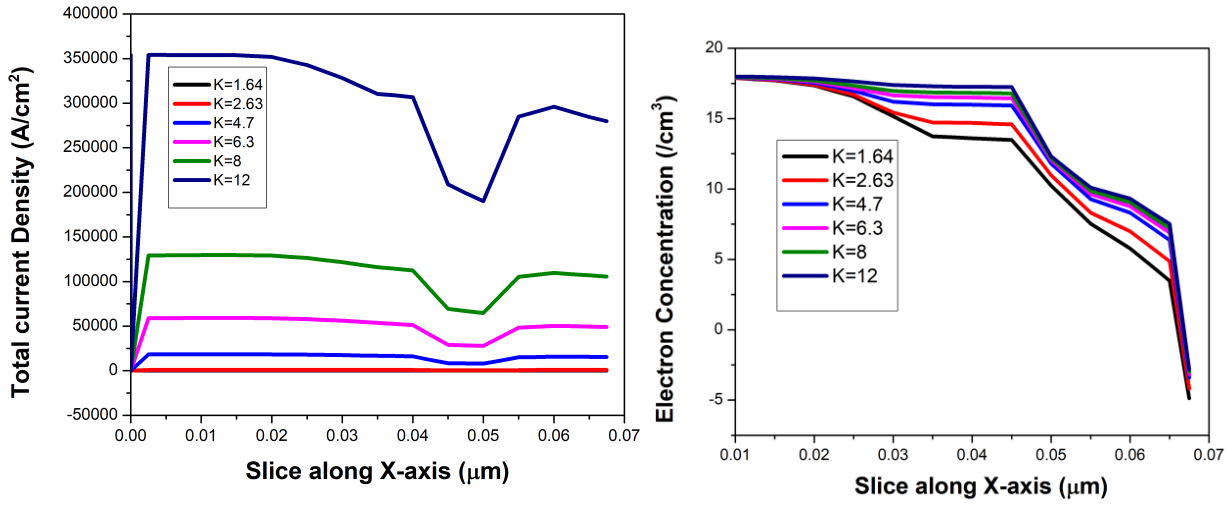

Figure 4.17 (a) Total current density (b) Electron Concentration with respect to different biomolecules

Biosensor sensitivity plays a crucial role in the accurate and precise detection of target molecules or analytes. As the permittivity of the cavity in a biosensor increased, it significantly impacts the device's sensitivity. The permittivity, which represents the material's ability to store electrical energy, influences the electric field distribution within the cavity. The sensitivity of the biomolecules is calculated with the help of below expression:

$$S_I = \frac{I_D(\text{bio}) - I_D(\text{air})}{I_D(\text{air})} - - - - - - 4.3$$

In Figure 4.18, the sensitivity of the neutral biomolecules increasing when the k value is increasing, the increment of k value also results in high electric field concentration in the cavity leading to enhance interactions between the sensing surface and target analyte.

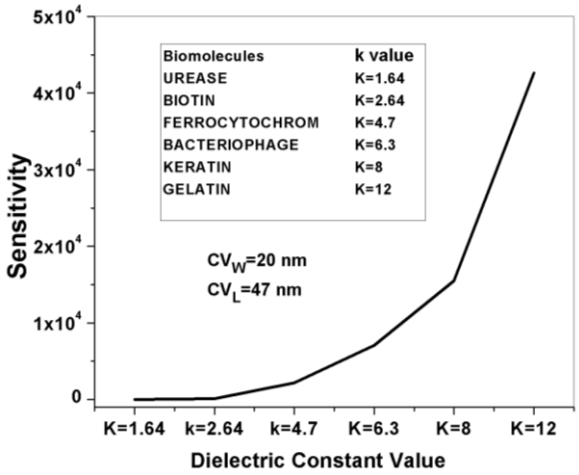

Figure 4.18: **Sensitivity of Biomolecules**

Furthermore, the surface-to-volume ratio of the cavity also plays a critical role in biosensor sensitivity. The increased surface area allows for mole binding sites and greater availability of active sites for analyte interactions. Consequently, it enhances the chance of successful analyte binding, leading to improved sensitivity of biosensor.

The combination of increased permittivity and higher surface to volume ratio in the cavity result in a synergistic effort on biosensor sensitivity. The presence of high electric field due to increased permittivity, along with the larger sensing area produced by the higher surface to volume ratio, enable enhanced analyte binding and more effective signal transduction.

4.5 Effect of cavity Filling level on drain current

The impact of the height t_{gap} of the cavity on drain current is shown in Figure 4.19. For a fixed value of the K, higher the thickness lower will be C_{gap}. Thus, reducing the effective capacitance (C_{gap}). And hence the variation of I_{ON} becomes less. Further, for higher value of cavity thickness (t_{gap}) I_{OFF} reduces and as such the I_{ON}/I_{OFF} ratio increases. From Figure 4.19, it can be observed clearly that even in sub-threshold regime, when t_{gap} lies between $6nm \leq t_{gap} \leq 10nm$ I_{ON}/I_{OFF} ratios goes nearly 10^8

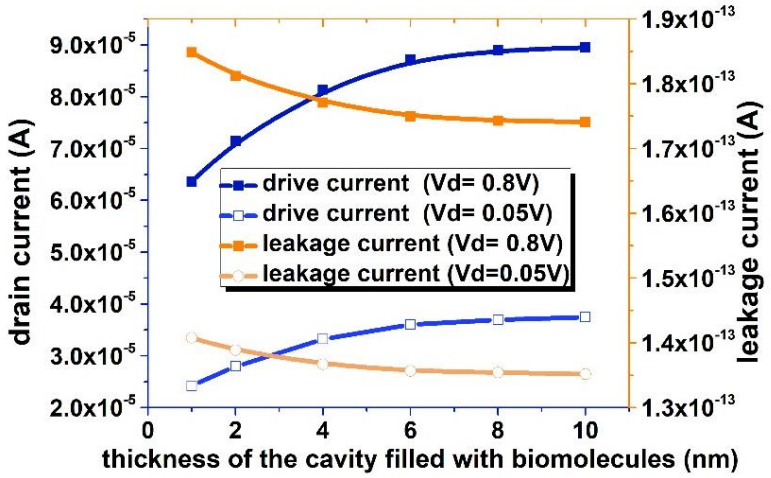

Figure 4.19 Variation of drain current with respect to the height thickness of the cavity filled with biomolecules

4.6 Analysis of Gate on source Tubular tunnel FET based biosensor

In this section the silicon nanotube-based biosensors results are going to be discussed. For all the simulation the drain current is taken as 1V and both aluminum and tungsten are employed as a gate electrode. There are two types of techniques in biosensors i.e., gating and dielectric modulated. In this work we have utilized the dielectric modulated type biosensor to realize the different type of biomolecules. To realize the enzymes, proteins and other biomolecules, values ranging from 1 to 9 for the dielectric constant is considered. Figure 4.20 shows the potential contour of tubular based biosensor at k=9. As we observed Potential is maximum at the gate electrodes but as we are moving the silicon region the potential is changing and when we immobilize with different dielectric constant values than we are getting the sufficient difference so we can able to discriminate between the different types of biomolecules.

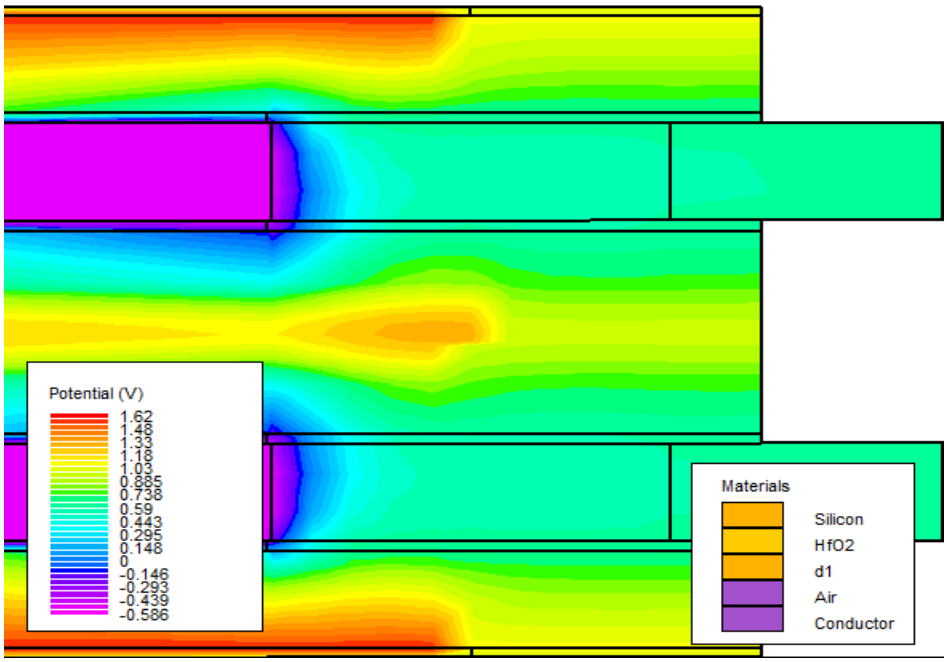

Figure 4.20. Potential contour of Silicon nanotube tunnel FET biosensor

Figure 4.21 shows transfer characteristics of tubular based biosensor. It is observed from Figure 4.21 that on increasing the value of k, drain current is increasing and there is a vast change in the I_{ON} current as well as subthreshold swing. On increasing the k value from 3 to 7 the drain current is changing about 10^2 folds, which is comparatively good among the other sensitivity parameter.

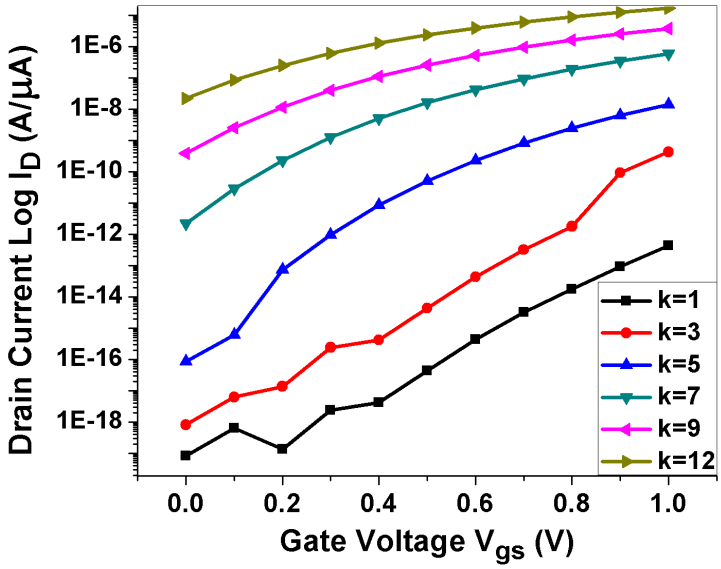

Figure 4.21 Transfer Characteristic of Silicon nanotube tunnel FET based biosensor with different k values

Figure 4.22 (a) depicts the impact of k values varying from 1 to 9 on vertical electric field along with X axis and Figure 4.22(b) presents the effect of different k value on the electron

mobility in x direction. It is observed from the Figure 4.22 (a) that on escalating the k value the vertical electric field is actually increasing in -ve direction and the electron mobility is also decreasing on increasing the value of k. Actually, electron mobility has to increase but the figure shows the electron mobility, which is perpendicular to the structure.

The electron concentration is also one of the major parameters while working on FET based sensors. The impact of k value on the electron concentration inside the silicon region is shown in Figure 4.22. The electron concentration is slight increasing at the larger value of k but at the smaller value of k the variation in the electron concentration at the source channel region is very high.

Finally, to check the sensitivity of biosensor, calculation of sensitivity parameter is very important. The drain current was used as a sensitivity parameter in this work. The sensitivity is determined by following formula and the found values are written in the Table 4.3.

$$S_I = \frac{I_D(bio) - I_D(air)}{I_D(air)} - - - - - 4.4$$

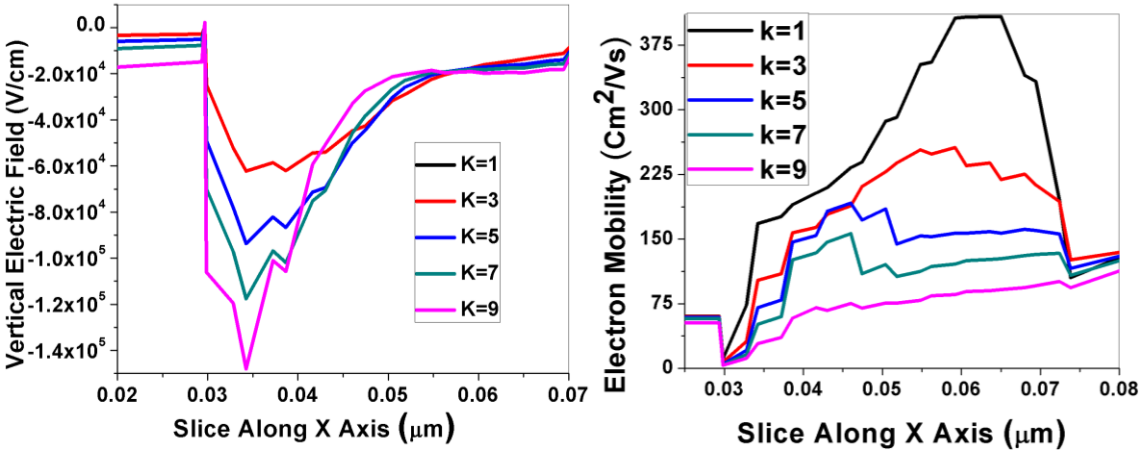

Figure 4.22 (a) Vertical Electric Field (b) Electron Mobility Potential contour of Silicon nanotube tunnel FET biosensor

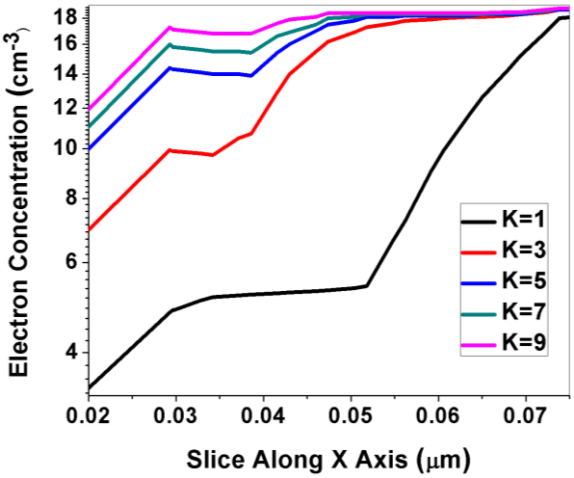

Figure.4.23 Impact of K value on Electron concentration along X axis.

As the values of the k increasing the sensitivity is also increasing, for example k=3 the sensitivity in 10^2 but when the value is increasing to k=9 the sensitivity is in 10^6. The main benefit of this structure is that more biomolecules can immobilize on the surface since there is increased surface area relative to volume, that is, both within and outside the tube.

Table 4.3. Sensitivity values

K=1	0.00E+00
K=3	9.99E+02
K=5	3.29E+04
K=7	1.36E+06
K=9	8.79E+06
K=12	3.92E+07

4.7 Reduction of Short channel Effect in FET devices

As shown in Figure 4.24 the fringes electric field are more in single gate MOS compare to double gate MOS device. Because in double gate device due to the presence of two gates the electric field lines are not entering towards. In double gate the channel is electrically shielded from the charge originated due to the drain bias. The drive capability is more and the leakage current is drastically reduced, this is due to the excellent electrostatic coupling. In double gate MOS the threshold voltage is also possible to control using increment in the body doping, utilization of the metal gate, through work function engineering the desired threshold voltage can be possible to achieve. Due to the reduced channel and gate leakage in OFF state, the power saving is also more. Double gate devices are very promising for the circuit design in sub 50 nm technology node.

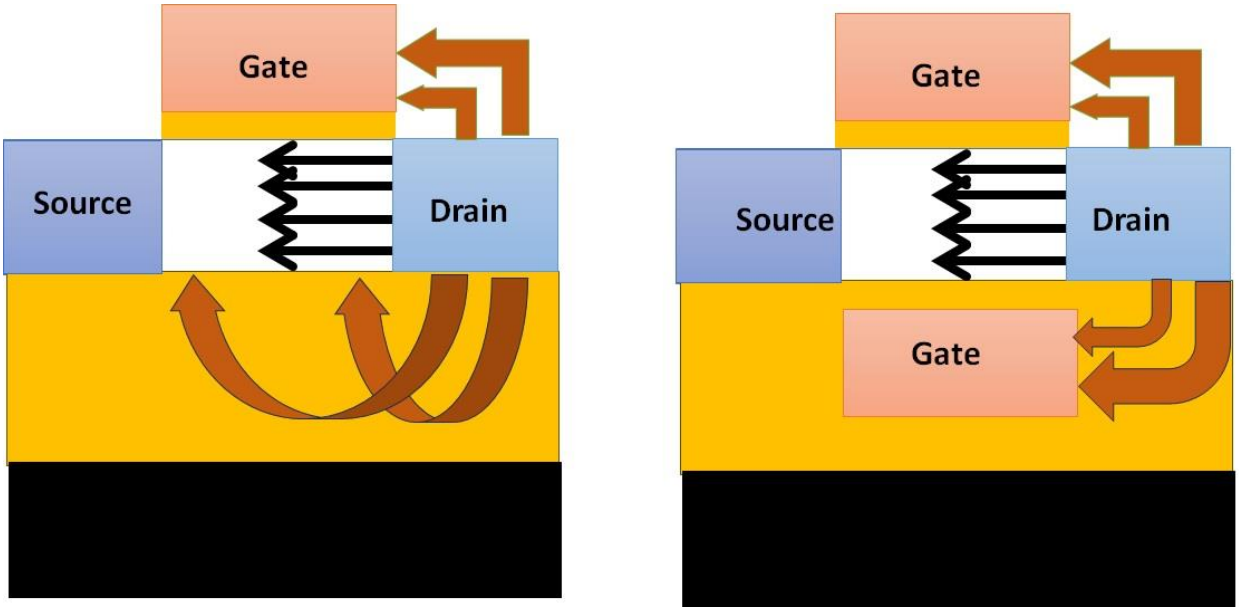

Figure.4.24 Single Gate FET vs Double gate FET

Another structure which we have utilized in this thesis for simulating the biosensor is junction less TFET. Some properties of the junction less TFET are discussed below:

- Without P-N Junction
- Carrier modulation is controlled by the gate work function and gate voltage
- High doping
- No doping gradient
- Normally ON state device
- Surface based conduction

When the source and drain of a conventional FET partially overlap the gate, short-channel effects like DIBL and a deteriorated subthreshold slope result from the lateral expansion of the S/D depletion charges in the channel area. In a JLT, these are not present due to the absence of junction these FETs have good subthreshold slope and DIBL and are less susceptible to short-channel effects than devices with junctions. The comparison between MOSFET in inversion state and junction less FET is given in Table 4.4

Table 4.4: Comparison between MOSFET and Junction less FET

Parameter	MOSFET (Inversion)	Junction-less TFET
Subthreshold slope	75 m V/decade	92 mV/decade
DIBL	10 mV/V	78 mV/V
I_{ON}	1000 µA/µm	1000 µA/µm
I_{ON}/I_{OFF}	$5x10^6$	$5x10^6$

CHAPTER FIVE

CONCLUSION

In this project work, dielectric modulation in embedded nanogap is exploited to achieve bio-sensing in a silicon nano tube-based FET (TFET) through a variation in device's drain current (ambipolar current) behavior. Biosensor has a maximum yield when a large number of biomolecules are able to immobilize on the surface and change the sensitivity parameter accordingly. It can be possible only when the surface to volume (S/V) ratio is maximum. The S/V ratio is maximum in tubular devices as compared to other FET devices. An overview of the sensitivities of existing biosensors reveals that the silicon tube-based devices have the ability to perform as a satisfactory biosensor in subthreshold regime. So, the proposed device can be a good alternative to other biosensors for label-free detection of neutral biomolecules as well as charged ones.

In this research work, three Different proposed structures i.e., Double Gate Both Side Cavity TFET, Double Gate Full both side Cavity TFET and Double Gate Drain side cavity TFET were discussed. We used the Kane model of tunneling to realize the band to band tunneling in all the simulations. The immobilization of the biomolecules in the cavity regions realize using the variation in dielectric constant and charge density. Further the energy band diagram, horizontal and vertical electric fields, transfer characteristics are observed to finally calculate the ambipolar current sensitivity, and I_{ON}/I_{OFF} ratio. The sensitivity and ambipolar current of the three proposed sensor are compared. The sensitivity of the DG-FBSC-TFET sensor is relatively high, which is very suitable for applications in the field of ultra-sensitivity, low consumption biosensors. DG-FBSC-TFET also shows better sensitivity and improved ambipolar current when compared with both DG-BSC-TFET and DG-DSC-TFET for biosensor application. Therefore, DG-FBSC-TFET sensor has insightful development potential and market views for future low power biosensors. In addition, we have utilized the heterojunction Junction less tunnel FET for biosensing application. The presence of Hetero-structure in the device improves mobility and the narrow band gap interface between the source and channel interfaces enhances the band-to band tunneling effect at channel-source interface. Here we used hafnium oxide as the gate oxide material. The high-k dielectric also enhances the capacitive effect of the gate and reduces the effective oxide thickness (EOT). The performance of dielectric modulated biosensor is analyzed by investigating the sensitivity by varying the k value of various biomolecules. To check the

insight performance of the FET based biosensor, the impact of different type of biomolecules on the electric fields, recombination rate and conduction current density is observed. It is concluded that the proposed device has better performance than the conventional device, particularly for the low power biosensing application.

Finally, we presented a silicon-based tubular Tunnel FET providing extremely sensitive biosensors. ON current (I_{ON}) or drain current is used as the sensitivity parameter. It was also found that device utilizing the TCAD tool that every time biomolecules connect to surfaces of the tubular FET, the intensity of the drain current varies, causing the tunnelling barrier width at the channel drain interface to fluctuate. The sensitivity of the proposed FET based biosensor is also more because of the overlapping gate on the source region. Sensitivity is measured for k= 1 to k=9 and it has been found on increasing the value of the k the sensitivity is also increased with noted amount.

Recommendation for the future is given below

- In the future, this form of biosensor might be used for low power DM FET-based biosensors
- The analytical modelling of threshold voltage, subthreshold slope, etc., can be done in future.
- Detailed circuit and RF analysis for proposed bio sensing devices.
- Optimize the biosensor performance for the subthreshold regime and also check the suitability for the charge biomolecules.
- Possible fabrication of the FET based biosensor for label free detection.

REFERENCES

[1] A. Singh, S. Adak, H. Pardeshi, A. Sarkar, and C. K. Sarkar, "Strained based FDSOI MOSFET slojem in na osnovi napetega silicija," vol. 45, no. 1, pp. 73–79, 2015.

[2] P. Hashemi, C. Science, J. L. Hoyt, T. Supervisor, and T. P. Orlando, "Gate-All-Around Silicon Nanowire MOSFETs : Top-down Fabrication and Transport Enhancement Techniques," *Electr. Eng.*, 2010.

[3] J. P. Colinge and A. Chandrakasan, *FinFETs and other multi-gate transistors*. 2008. doi: 10.1007/978-0-387-71752-4.

[4] A. Veloso, A. De Keersgieter, P. Matagne, N. Horiguchi, and N. Collaert, "Advances on doping strategies for triple-gate fi nFETs and lateral gate-all- around nanowire FETs and their impact on device performance," *Mater. Sci. Semicond. Process.*, vol. 62, no. July, pp. 0–1, 2016, doi: 10.1016/j.mssp.2016.10.018.

[5] X. Chen and C. M. Tan, "Modeling and analysis of gate-all-around silicon nanowire FET," *Microelectron. Reliab.*, vol. 54, no. 6–7, pp. 1103–1108, 2014, doi: 10.1016/j.microrel.2013.12.009.

[6] S. Sahay and M. J. Kumar, "A Novel Gate-Stack-Engineered Nanowire FET for Scaling to the Sub-10-nm Regime," *IEEE Trans. Electron Devices*, vol. 63, no. 12, pp. 5055–5059, 2016, doi: 10.1109/TED.2016.2617383.

[7] J. P. Colinge, "Multiple-gate SOI MOSFETs," *Solid. State. Electron.*, vol. 48, no. 6, pp. 897–905, 2004, doi: 10.1016/j.sse.2003.12.020.

[8] D. Tekleab, "Device performance of silicon nanotube field effect transistor," *IEEE Electron Device Lett.*, vol. 35, no. 5, pp. 506–508, 2014, doi: 10.1109/LED.2014.2310175.

[9] A. Singh, S. Chaudhury, C. K. Pandey, S. M. Sharma, and C. K. Sarkar, "Design and analysis of high k silicon nanotube tunnel FET device," *IET Circuits, Devices Syst.*, vol. 13, no. 8, pp. 1305–1310, 2019, doi: 10.1049/iet-cds.2019.0230.

[10] H. M. Fahad, C. E. Smith, J. P. Rojas, and M. M. Hussain, "Silicon nanotube field effect transistor with core-shell gate stacks for enhanced high-performance operation and area scaling benefits," *Nano Lett.*, vol. 11, no. 10, pp. 4393–4399, 2011, doi: 10.1021/nl202563s.

[11] A. Singh, S. Chaudhary, S. M. Sharma, and C. K. Sarkar, "Improved Drive Capability of

Silicon Nano Tube Tunnel FET Using Halo Implantation," *Silicon*, 2020, doi: 10.1007/s12633-019-00350-y.

[12] D. Sarkar and K. Banerjee, "Proposal for tunnel-field-effect-transistor as ultra-sensitive and label-free biosensors," *Appl. Phys. Lett.*, vol. 100, no. 14, 2012, doi: 10.1063/1.3698093.

[13] P. Bergveld, "The development and application of FET-based biosensors," *Biosensors*, vol. 2, no. 1, pp. 15–33, 1986, doi: 10.1016/0265-928X(86)85010-6.

[14] H. Im, X. Huang, B. Gu, and Y. Choi, "LETTERS A dielectric-modulated field-effect transistor for biosensing," vol. 2, no. July, 2007, doi: 10.1038/nnano.2007.180.

[15] C. H. Kim, J. H. Ahn, K. B. Lee, C. Jung, H. G. Park, and Y. K. Choi, "A new sensing metric to reduce data fluctuations in a nanogap-embedded field-effect transistor biosensor," *IEEE Trans. Electron Devices*, vol. 59, no. 10, pp. 2825–2831, 2012, doi: 10.1109/TED.2012.2209650.

[16] R. Narang, K. V. S. Reddy, M. Saxena, R. S. Gupta, and M. Gupta, "A Dielectric-Modulated Tunnel-FET-Based Biosensor for Label-Free Detection: Analytical Modeling Study and Sensitivity Analysis," *IEEE Trans. Electron Devices*, vol. 59, no. 10, pp. 2809–2817, 2012, doi: 10.1109/TED.2012.2208115.

[17] Y.-C. Syu, W.-E. Hsu, and C.-T. Lin, "Review—Field-Effect Transistor Biosensing: Devices and Clinical Applications," *ECS J. Solid State Sci. Technol.*, vol. 7, no. 7, pp. Q3196–Q3207, 2018, doi: 10.1149/2.0291807jss.

[18] M. Curreli *et al.*, "Real-Time, Label-Free Detection of Biological Entities Using Nanowire-Based FETs," *Ieee Trans. Nanotechnol.*, vol. 7, no. 6, pp. 651–667, 2008, doi: 10.1109/tnano.2008.2006165.

[19] P. Mehrotra, "Biosensors and their applications – A review," *J. Oral Biol. Craniofacial Res.*, vol. 6, no. 2, pp. 153–159, May 2016, doi: 10.1016/J.JOBCR.2015.12.002.

[20] P. S. Gupta, S. Kanungo, H. Rahaman, K. Sinha, and P. S. Dasgupta, "An Extremely Low Sub-Threshold Swing UTB SOI Tunnel-FET Structure Suitable for Low-Power Applications," *Int. J. Appl. Phys. Math.*, vol. 2, no. 4, pp. 240–243, 2012, doi: 10.7763/IJAPM.2012.V2.101.

[21] R. Narang and M. Gupta, "Investigation of Dielectric-Modulated Double-Gate Junctionless MOSFET For Detection of Biomolecules," no. December, 2013, doi: 10.1109/INDCON.2013.6725863.

[22] F. Yan and H. Tang, “Editorial: Application of thin-film transistors in label-free DNA biosensors,” *Expert Rev. Mol. Diagn.*, vol. 10, no. 5, pp. 547–549, 2010, doi: 10.1586/erm.10.50.

[23] Z. Ahangari, “Performance assessment of dual material gate dielectric modulated nanowire junctionless MOSFET for ultrasensitive detection of biomolecules,” *RSC Adv.*, vol. 6, no. 92, pp. 89185–89191, 2016, doi: 10.1039/c6ra17361f.

[24] C. Vu, “Field-E ff ect Transistor Biosensors for Biomedical,” p. 22, 2019.

[25] K. Roy, S. Mukhopadhyay, and S. Member, “Leakage Current Mechanisms and Leakage Reduction Techniques in Deep-Submicrometer CMOS Circuits,” vol. 91, no. 2, 2003.

[26] N. V. Karimi and Y. Pourasad, “Tunneling Carbon Nanotube Field Effect Transistor with Asymmetric Graded Double Halo Doping in Channel: Asym-GDH-T-CNTFET,” *Procedia Mater. Sci.*, vol. 11, pp. 287–292, 2015, doi: 10.1016/j.mspro.2015.11.064.

[27] H. Yamada *et al.*, “Ferroelectric control of a Mott insulator,” *Sci. Rep.*, vol. 3, no. 001, pp. 1–6, 2013, doi: 10.1038/srep02834.

[28] A. Saeidi, F. Jazaeri, I. Stolichnov, and A. M. Ionescu, “Double-Gate Negative-Capacitance MOSFET with PZT Gate-Stack on Ultra Thin Body SOI: An Experimentally Calibrated Simulation Study of Device Performance,” *IEEE Trans. Electron Devices*, vol. 63, no. 12, pp. 4678–4684, 2016, doi: 10.1109/TED.2016.2616035.

[29] Y. X. Liu *et al.*, “Flexible threshold voltage FinFETs with independent double gates and an ideal rectangular cross-section Si-Fin channel,” *IEEE Int. Electron Devices Meet. 2003*, vol. 247, no. 2002, pp. 986–988, 2003, doi: 10.1109/IEDM.2003.1269445.

[30] S. Zhang, “Review of Modern Field Effect Transistor Technologies for Scaling,” *J. Phys. Conf. Ser.*, vol. 1617, no. 1, pp. 0–8, 2020, doi: 10.1088/1742-6596/1617/1/012054.

[31] S. Chen, H. Liu, S. Wang, W. Li, X. Wang, and L. Zhao, “Analog/RF Performance of T-Shape Gate Dual-Source Tunnel Field-Effect Transistor,” *Nanoscale Res. Lett.*, vol. 13, 2018, doi: 10.1186/s11671-018-2723-y.

[32] N. Mohankumar, B. Syamal, and C. K. Sarkar, “Investigation of novel attributes of single halo dual-material double gate MOSFETs for analog/RF applications,” *Microelectron. Reliab.*, vol. 49, no. 12, pp. 1491–1497, Dec. 2009, doi: 10.1016/j.microrel.2009.06.006.

[33] C. Rajan, D. P. Samajdar, and A. Lodhi, “Investigation of DC, RF and Linearity Performances of III–V Semiconductor-Based Electrically Doped TFET for Mixed Signal Applications,” *J. Electron. Mater.*, vol. 50, no. 4, 2021, doi: 10.1007/s11664-021-08753-

7.

[34] A. Kuamr, N. Chatterjee, S. Pandey, U. Kardam, and M. Gupta, “Analytical modeling and simulation based investigation of advanced TFET architecture,” in *Proceedings - 2016 International Conference on Micro-Electronics and Telecommunication Engineering, ICMETE 2016*, Institute of Electrical and Electronics Engineers Inc., Jul. 2016, pp. 523–528. doi: 10.1109/ICMETE.2016.90.

[35] R. Goswami, “Gate Engineered and Bandgap Engineered TFETs : simulation , modeling and applications Department of Electronics and Communication Engineering National Institute of Technology Silchar,” no. 14, 2017.

[36] Silvaco Inc., “Atlas User’s Manual,” *Silvaco Inc.*, no. 408, p. 1715, 2016, [Online]. Available: https://dynamic.silvaco.com/dynamicweb/jsp/downloads/DownloadManualsAction.do?req=silen-manuals&nm=atlas

[37] M. Yadav, A. Bulusu, and S. Dasgupta, “Super-threshold semi analytical channel potential model for DG tunnel FET,” *J. Comput. Electron.*, pp. 566–573, 2015, doi: 10.1007/s10825-015-0679-z.

[38] W. Huang *et al.*, “Investigation of Negative DIBL Effect and Miller Effect for Negative Capacitance Nanowire Field-Effect-Transistors,” *IEEE J. Electron Devices Soc.*, vol. 8, no. June, pp. 879–884, 2020, doi: 10.1109/JEDS.2020.3015492.

[39] A. Z. Laser *et al.*, “Multi-gate Si nanowire MOSFETs : Fabrication , strain engineering and transport analysis,” *IEEE Trans. Electron Devices*, vol. 63, no. 3, pp. 1689–1699, 2013, doi: 10.1017/CBO9781107415324.004.

[40] K. Boucart and A. M. Ionescu, “Double Gate Tunnel FET with ultrathin silicon body and high-k gate dielectric,” no. Imm, pp. 383–386, 2006.

[41] Ashita, S. A. Loan, and M. Rafat, “A High-Performance Inverted-C Tunnel Junction FET with Source-Channel Overlap Pockets,” *IEEE Trans. Electron Devices*, vol. 65, no. 2, pp. 763–768, 2018, doi: 10.1109/TED.2017.2783764.

[42] S. Saxena, S. L. Tripathi, S. K. Sinha, G. S. Patel, and C. Pravalika, “Review on Performance Evaluation of Tfet Structures & Its Applications Review on Performance Evaluation of Tfet Structures & Its Applications,” *Rev. Perform. Eval. Tfet Struct. Its Appl.*, no. May 2020, 2019.

[43] D. B. Abdi and M. J. Kumar, “Controlling ambipolar current in tunneling FETs using

overlapping gate-on-drain," *IEEE J. Electron Devices Soc.*, vol. 2, no. 6, pp. 187–190, 2014, doi: 10.1109/JEDS.2014.2327626.

[44] I. A. Pindoo, S. K. Sinha, and S. Chander, "Improvement of Electrical Characteristics of SiGe Source Based Tunnel FET Device," *Silicon*, vol. 13, no. 9, pp. 3209–3215, 2021, doi: 10.1007/s12633-020-00674-0.

[45] S. B. Rahi, P. Asthana, and S. Gupta, "Heterogate junctionless tunnel field-effect transistor: future of low-power devices," *J. Comput. Electron.*, vol. 16, no. 1, pp. 30–38, 2017, doi: 10.1007/s10825-016-0936-9.

[46] S. Wang *et al.*, "Device simulation of GeSn/GeSiSn pocket n-type tunnel field-effect transistor for analog and RF applications," *Superlattices Microstruct.*, vol. 111, pp. 286–292, Nov. 2017, doi: 10.1016/j.spmi.2017.06.037.

[47] B. V. V. Satyanarayana and M. D. Prakash, "Lower subthreshold swing and improved miller capacitance heterojunction tunneling transistor with overlapping gate," *Mater. Today Proc.*, vol. 45, no. xxxx, pp. 1997–2001, 2021, doi: 10.1016/j.matpr.2020.09.420.

[48] B. R. Raad, D. Sharma, P. Kondekar, K. Nigam, and S. Baronia, "DC and analog/RF performance optimisation of source pocket dual work function TFET," *Int. J. Electron.*, vol. 104, no. 12, pp. 1992–2006, Dec. 2017, doi: 10.1080/00207217.2017.1335788.

[49] R. Dutta, T. D. Subash, and N. Paitya, "Improved DC Performance Analysis of a Novel Asymmetric Extended Source Tunnel FET (AES-TFET) for Fast Switching Application," *Silicon*, 2021, doi: 10.1007/s12633-021-01147-8.

[50] C. Li, X. Zhao, Y. Zhuang, Z. Yan, J. Guo, and R. Han, "Optimization of L-shaped tunneling field-effect transistor for ambipolar current suppression and Analog/RF performance enhancement," *Superlattices Microstruct.*, vol. 115, pp. 154–167, Mar. 2018, doi: 10.1016/j.spmi.2018.01.025.

[51] J. P. Colinge *et al.*, "Junctionless Transistors: Physics and Properties," *Eng. Mater.*, no. February, pp. 187–200, 2011, doi: 10.1007/978-3-642-15868-1_10.

[52] S. Sahay and M. J. Kumar, *Modeling Junctionless Field-Effect Transistors*. 2019. doi: 10.1002/9781119523543.ch8.

[53] M. Rahimian and M. Fathipour, "Asymmetric junctionless nanowire TFET with built-in n+ source pocket emphasizing on energy band modification," *J. Comput. Electron.*, vol. 15, no. 4, pp. 1297–1307, 2016, doi: 10.1007/s10825-016-0895-1.

[54] M. Rahimian and M. Fathipour, "Improvement of electrical performance in junctionless

nanowire TFET using hetero-gate-dielectric," *Mater. Sci. Semicond. Process.*, vol. 63, no. November 2016, pp. 142–152, 2017, doi: 10.1016/j.mssp.2016.12.011.

[55] U. Ragavendran and M. Ramachandran, "Low power and low area junction-less tunnel FET design," *Int. J. Eng. Technol.*, vol. 7, no. 3.1 Special Issue 1, pp. 155–157, 2018, doi: 10.14419/ijet.v7i3.1.17076.

[56] B. Ghosh and M. W. Akram, "Junctionless tunnel field effect transistor," *IEEE Electron Device Lett.*, vol. 34, no. 5, pp. 584–586, 2013, doi: 10.1109/LED.2013.2253752.

[57] Mahalaxmi, B. Acharya, and G. P. Mishra, "Design and Analysis of Dual-Metal-Gate Double-Cavity Charge-Plasma-TFET as a Label Free Biosensor," *IEEE Sens. J.*, vol. 20, no. 23, pp. 13969–13975, 2020, doi: 10.1109/JSEN.2020.2979016.

[58] P. Bergveld, "Thirty years of ISFETOLOGY," *Sensors Actuators B Chem.*, vol. 88, no. 1, pp. 1–20, 2003, doi: 10.1016/S0925-4005(02)00301-5.

[59] N. Bhalla, P. Jolly, N. Formisano, and P. Estrela, "Introduction to biosensors," *Essays Biochem.*, vol. 60, no. 1, pp. 1–8, 2016, doi: 10.1042/EBC20150001.

[60] R. Narang, S. Member, M. Saxena, and S. Member, "Dielectric Modulated Tunnel Field-Effect Transistor — A Biomolecule Sensor," vol. 33, no. 2, pp. 266–268, 2012.

[61] X. P. A. Gao, G. Zheng, and C. M. Lieber, "Subthreshold regime has the optimal sensitivity for nanowire FET biosensors," *Nano Lett.*, vol. 10, no. 2, pp. 547–552, 2010, doi: 10.1021/nl9034219.

[62] D. Sung and J. Koo, "A review of BioFET's basic principles and materials for biomedical applications," *Biomed. Eng. Lett.*, vol. 11, no. 2, pp. 85–96, 2021, doi: 10.1007/s13534-021-00187-8.

[63] C. Kim, C. Jung, H. G. Park, and Y. Choi, "Novel Dielectric-Modulated Field-Effect Transistor for Label-Free DNA Detection," vol. 2, no. 2, pp. 127–134, 2008.

[64] S. Sang, Y. Wang, Q. Feng, Y. Wei, J. Ji, and W. Zhang, "Progress of new label-free techniques for biosensors : a review," *Crit. Rev. Biotechnol.*, vol. 00, no. 00, pp. 1–17, 2015, doi: 10.3109/07388551.2014.991270.

[65] N. N. Reddy and D. K. Panda, "A Comprehensive Review on Tunnel Field-Effect Transistor (TFET) Based Biosensors: Recent Advances and Future Prospects on Device Structure and Sensitivity," *Silicon*, vol. 13, no. 9, pp. 3085–3100, 2021, doi: 10.1007/s12633-020-00657-1.

[66] M. Zhang, Y. Guo, J. Zhang, J. Yao, and J. Chen, "Simulation Study of the Double-Gate

Tunnel Field-Effect Transistor with Step Channel Thickness," *Nanoscale Res. Lett.*, vol. 15, no. 1, 2020, doi: 10.1186/s11671-020-03360-7.

[67] S. Kanungo, S. Chattopadhyay, P. S. Gupta, and H. Rahaman, "Comparative performance analysis of the dielectrically modulated full- gate and short-gate tunnel FET-based biosensors," *IEEE Trans. Electron Devices*, vol. 62, no. 3, pp. 994–1001, 2015, doi: 10.1109/TED.2015.2390774.

[68] P. Venkatesh, K. Nigam, S. Pandey, D. Sharma, and P. N. Kondekar, "A dielectrically modulated electrically doped tunnel FET for application of label free biosensor," *Superlattices Microstruct.*, vol. 109, pp. 470–479, 2017, doi: 10.1016/j.spmi.2017.05.035.

[69] M. Verma, S. Tirkey, S. Yadav, D. Sharma, and D. S. Yadav, "Performance Assessment of A Novel Vertical Dielectrically Modulated TFET-Based Biosensor," *IEEE Trans. Electron Devices*, vol. 64, no. 9, pp. 3841–3848, Sep. 2017, doi: 10.1109/TED.2017.2732820.

[70] A. Singh, S. Chaudhury, M. Chanda, and C. K. Sarkar, "Split gated silicon nanotube FET for biosensing applications," *IET Circuits, Devices Syst.*, vol. 14, no. 8, pp. 1289–1294, 2020, doi: 10.1049/iet-cds.2020.0208.

[71] A. Singh, C. K. Pandey, S. Chaudhury, and C. K. Sarkar, "Effect of strain in silicon nanotube FET devices for low power applications," *EPJ Appl. Phys.*, vol. 85, no. 1, 2019, doi: 10.1051/epjap/2018180236.

[72] V. Vijayvargiya and S. K. Vishvakarma, "Effect of Drain Doping Profile on Double-Gate Tunnel Field-Effect Transistor and its Influence on Device RF Performance," *IEEE Trans. Nanotechnol.*, vol. 13, no. 5, pp. 974–981, Sep. 2014, doi: 10.1109/TNANO.2014.2336812.

[73] X. Liu, H. Hu, H. Zhang, B. Wang, J. Yang, and G. Han, "Study of drain induced barrier lowering (DIBL) effect and subthreshold characteristics of fully-depleted Ge NMOS with P-substrate," *Superlattices Microstruct.*, vol. 100, pp. 1230–1237, Dec. 2016, doi: 10.1016/j.spmi.2016.11.006.

[74] R. Dutta, N. Paitya, and A. Majumdar, "Ambipolar Reduction Methodology for SOI Tunnel FETs in Low Power Applications: A Performance Report," *Int. J. Recent Technol. Eng.*, vol. 8, no. 5, pp. 1894–1897, 2020, doi: 10.35940/ijrte.e6271.018520.

[75] D. Singh, S. Pandey, K. Nigam, D. Sharma, D. S. Yadav, and P. Kondekar, "A charge-plasma-based dielectric-modulated junctionless TFET for biosensor label-free detection,"

IEEE Trans. Electron Devices, vol. 64, no. 1, pp. 271–278, Jan. 2017, doi: 10.1109/TED.2016.2622403.

[76] S. Anand, A. Singh, S. I. Amin, and A. S. Thool, "Design and Performance Analysis of Dielectrically Modulated Doping-Less Tunnel FET-Based Label Free Biosensor," *IEEE Sens. J.*, vol. 19, no. 12, pp. 4369–4374, 2019, doi: 10.1109/JSEN.2019.2900092.

[77] C. Chong, H. Liu, S. Wang, S. Chen, and H. Xie, "micromachines Sensitivity Analysis of Biosensors Based on a Dielectric-Modulated L-Shaped Gate Field-Effect Transistor," 2020, doi: 10.3390/mi1201.

[78] D. M. T. Biosensor, M. Verma, S. Tirkey, S. Yadav, D. Sharma, and D. S. Yadav, "Performance Assessment of A Novel Vertical," pp. 1–8, 2017.

[79] I. Tahi, M. N. Rezaie, and R. Article, "Design and Simulation of InP and Silicon Nanowires With Different Channel Characteristic as Biosensors to Improve Output Sensitivity," pp. 0–24, 2018.

[80] Z. Ahangari, "Performance assessment of dual material gate dielectric modulated nanowire junctionless MOSFET for ultrasensitive detection of biomolecules," *RSC Adv.*, vol. 6, no. 92, pp. 89185–89191, 2016, doi: 10.1039/c6ra17361f.

APPENDIX A: PUBLICATIONS

A. Published

Journal Paper:

Solomon K. Jorga, et.al, "Comparative Analysis of Dielectric Engineered Tunnel FET for Biosensing Applications" September 2022, Silicon 15(8), DOI: 10.1007/s12633-022-02107-6

Conference Paper:

Avtar Singh et.al. "Study of Gate on Source based tubular TFET for biosensing Application" presented in ICICASEE-2023 1st International Conference on Intelligent Computation and Analytics on Sustainable Energy and Environment held at Ghani Khan Choudhury Institute of Engineering & Technology, Malda, W.B-732141, India

B. Under process

Journal Paper:

Avtar Singh et.al., "Assessment of Hetero-structure Junction-less Tunnel FET's efficacy for biosensing applications" Sensing and Imaging, Springer,2022 (under review)

APPENDIX B: GRADUATE STUDENTS BENEFITED FROM RESEARCH PROJECT

S.No	Name of Graduate Student	Thesis Title	Thesis Result
1	Ashebir Taressa Angesa	Design and Optimization of Tunnel Field-Effect Transistor using Dielectric Engineering for Analog/RF Amplification	Excellent
2	Solomon Kebede Jorga	Study And Analysis Of Dielectric Modulated FET Based Biosensors	Very Good
3	Rabiya Abdulnassir	Design and optimization of Junction less nanowire tunnel FET For low power Analog applications	Very Good

APPENDIX C: BUDGET UTILIZED

S.No	Items	Total Cost (ETB)	Remark
1	Perdiem for researchers	724ETB*30days*3person= 65,160.00	Utilized
2	Payments for Assistance	65ETB*20days*8hours*3person = 31,200.00	Utilized
3	Car rent	2500ETB*15days = 37,500.00	Utilized
4	GPU based Laptop	51,700.00	Utilized, budget added due to inflation
5	Digital Drawing Pen Tablet	4,150.00	Utilized
	Total utilized Budget	**189,710.00**	